US Army Corps of Engineers
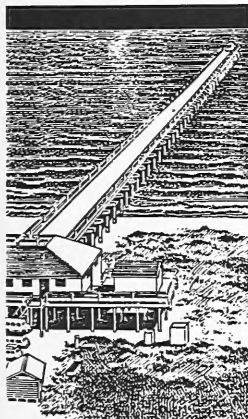
EXTREMAL ANALYSIS OF HINDCAST AND MEASURED WIND AND WAVE DATA AT KODIAK, ALASKA

by

Michael E. Andrew, Orson P. Smith
Jane M. McKee

Coastal Engineering Research Center

DEPARTMENT OF THE ARMY
Waterways Experiment Station, Corps of Engineers
PO Box 631
Vicksburg, Mississippi 39180-0631

June 1985
Final Report

REPORT DOCUMENTATION PAGE		READ INSTRUCTIONS BEFORE COMPLETING FORM
1. REPORT NUMBER Technical Report CERC-85-4	2. GOVT ACCESSION NO.	3. RECIPIENT'S CATALOG NUMBER
4. TITLE *(and Subtitle)* EXTREMAL ANALYSIS OF HINDCAST AND MEASURED WIND AND WAVE DATA AT KODIAK, ALASKA		5. TYPE OF REPORT & PERIOD COVERED Final report
		6. PERFORMING ORG. REPORT NUMBER
7. AUTHOR(s) Michael E. Andrew Orson P. Smith Jane M. McKee		8. CONTRACT OR GRANT NUMBER(s)
9. PERFORMING ORGANIZATION NAME AND ADDRESS US Army Engineer Waterways Experiment Station Coastal Engineering Research Center PO Box 631, Vicksburg, Mississippi 39180-0631		10. PROGRAM ELEMENT, PROJECT, TASK AREA & WORK UNIT NUMBERS
11. CONTROLLING OFFICE NAME AND ADDRESS US Army Engineer District, Alaska Pouch 898, Anchorage, Alaska 99506		12. REPORT DATE June 1985
		13. NUMBER OF PAGES 75
14. MONITORING AGENCY NAME & ADDRESS*(if different from Controlling Office)*		15. SECURITY CLASS. *(of this report)* Unclassified
		15a. DECLASSIFICATION/DOWNGRADING SCHEDULE

16. DISTRIBUTION STATEMENT *(of this Report)*

Approved for public release; distribution unlimited.

17. DISTRIBUTION STATEMENT *(of the abstract entered in Block 20, if different from Report)*

18. SUPPLEMENTARY NOTES

19. KEY WORDS *(Continue on reverse side if necessary and identify by block number)*

Ocean waves--Measurement (LC)   Water wave hindcasting (WES)
Winds--Alaska--Measurement (LC)
St. Paul Harbor (Kodiak, Alaska) (LC)
Wind waves--Alaska--Measurement (LC)

20. ABSTRACT *(Continue on reverse side if necessary and identify by block number)*

    The purpose of this study is to provide an analysis of hindcast and mea-
sured wave and wind data to estimate the long-term extreme wave heights for
the St. Paul Harbor area at Kodiak, Alaska. This study included the develop-
ment of the deepwater extreme wave climate, the derivation of a wave energy
attenuation factor for deep- to shallow-water transition of extreme waves,

(Continued)

DD FORM 1473 1 JAN 73   EDITION OF 1 NOV 65 IS OBSOLETE

20.   ABSTRACT (Continued):

and an analysis of collateral wind data to support the results of the analysis
of hindcast wave data.

        The Wave Information Study (WIS) hindcast data applicable to the Kodiak
area was surveyed for extreme wave conditions.   This survey resulted in a
sample of 62 significant wave heights for the years 1956 through 1975 (Appen-
dix A).   The 62 significant wave heights were scaled and plotted according to
several extreme probability models.   The Extremal Type I or Fisher-Tippett
Type I model demonstrated a better fit with the data than did the other models
(Figure 1).   Extrapolated significant wave heights based on the Extremal
Type I model are listed versus return period in Table 7.   The extreme wave
predictions computed using monthly maximum significant wave height values from
measured wave data (Table 9) tended to be smaller than the hindcast predic-
tions.   This difference was best explained by the fact that the measured data
covered a time span of about 2 years; whereas, the hindcast data represented
20 years of wave climate.   The longer record had a better chance of capturing
a representative sample of extreme events than the short record.

        Extreme wave heights computed with long-term wind data provided by the
National Weather Service agreed well with results from the analysis of WIS
hindcast data and supported the overall validity of the study.

        Measured wave data provided by the Alaska Coastal Data Collection Pro-
gram were analyzed to obtain a wave energy attenuation factor for the long-
period swell crossing the reefs into St. Paul Harbor at Kodiak.   The atten-
uation factor represented the fraction of deepwater wave energy that is not
dissipated in the transition across the reefs into St. Paul Harbor.   The at-
tenuation factor had a value of 0.374; therefore, a significant wave height
of 1 m in deep water corresponded to 0.374 m inside the harbor.

        The long-term extreme wave height prediction from the analysis of hind-
cast data was adjusted to represent the long-term wave climate inside St. Paul
Harbor by means of the attenuation factor.   Values for attenuated long-term
significant wave heights are listed in Table 24.   These estimates represented
the best estimates for the extreme wave climate at St. Paul Harbor, based on
analyses of all the presently available data.

PREFACE

Authority for the US Army Engineer Waterways Experiment Station (WES) to conduct this study was contained in Intra-Army Order for Reimbursable Services No. E86-84-0018, dated 8 February 1984. The study was sponsored by the Alaska District Office of the Corps of Engineers, NPAEN-DL-P.

The study was conducted by personnel of the Coastal Engineering Research Center (CERC), WES, under the direction of Dr. R. W. Whalin, Chief, CERC, and Dr. F. E. Camfield, Acting Chief, Engineering Development Division. The study was performed under the direct supervision of Dr. Dennis R. Smith, Chief, Prototype Measurement and Analysis Branch, and Dr. Michael E. Andrew, assisted by Mr. Orson P. Smith and Ms. Jane M. McKee.

Commanders and Directors of WES during the conduct of the study and the preparation of this report were COL Tilford C. Creel, CE, and COL Robert C. Lee, CE. COL Allen F. Grum, CE, was Director of WES during the publication of this report. Technical Directors were Mr. Fred. R. Brown and Dr. Robert W. Whalin.

1

CONTENTS

CONVERSION FACTORS, NON-SI TO SI (METRIC)
UNITS OF MEASUREMENT

Non-SI units of measurement used in this report can be converted to SI (metric) units as follows:

Multiply	By	To Obtain
feet	0.3048	metres
miles (US nautical)	1.852	kilometres
miles (US statute)	1.609347	kilometres
square miles (US statute)	2589.988	square kilometres
yards	0.9144	metres

EXTREMAL ANALYSIS OF HINDCAST AND MEASURED
WIND AND WAVE DATA AT KODIAK, ALASKA

PART I: INTRODUCTION

Purpose of Study

1. This study was conducted to provide an analysis of hindcast and measured wave and wind data for Kodiak, Alaska. The purpose of the analysis was to obtain long-term extreme wave conditions for the St. Paul Harbor at Kodiak. This study was accomplished by means of extremal analyses of deep-water hindcast data from the nearest Wave Information Study (WIS) grid point outside Chiniak Bay. Long-term wind measurements were used to validate the results obtained from the analyses of the hindcast data. The local wave climate and attenuation factor for swell crossing the reef into St. Paul Harbor were derived using measured wave data from the area.

Physical Description of Kodiak and Vicinity

2. The city of Kodiak is located on the northeastern shore of Kodiak Island, on the western Gulf of Alaska, about 1,250 air miles* northwest of Seattle and 250 miles southwest of Anchorage. Kodiak Island is 3,588 square miles in area and is mostly mountainous terrain rising to over 4,000 ft in places. Its shoreline is characterized by deep glacial fiords separated by rocky peninsulas and many smaller islands. The center of the city lies on the Kodiak Island side of a narrow channel defined by Near Island. The Port of Kodiak's deep-draft facilities are southwest of the city on the northwest shore of that 50- to 60-ft-deep area of Chiniak Bay known as St. Paul Harbor. St. Paul Harbor is defined by a series of small islands and submerged rocky reefs a few feet deep extending from the offshore side of Near Island 2 miles to the southwest to just beyond Puffin Island. Further to the southwest of St. Paul Harbor is Womens Bay, the site of the US Coast Guard Kodiak Air

---

* A table of factors for converting non-SI units of measurement to SI (metric) units is presented on page 3.

Station. Chiniak Bay, offshore of the city and St. Paul Harbor, is defined by Cape Chiniak and Long Island and is exposed to the northern half of the Gulf of Alaska. Cape Chiniak offers protection from the Pacific Ocean to the south.

3. The specific area of interest to this study is the deep-draft terminal operated by the Port of Kodiak on St. Paul Harbor. This container dock is fully exposed to St. Paul Harbor, and its operations are intermittently disrupted by long-period swell which passes during bad weather over the reefs defining St. Paul Harbor.

4. Developments by the State of Alaska in Dog Bay on the southwest side of Near Island are under way; they were proposed in 1976 by the Corps of Engineers and are also of interest in this study. Dog Bay is sheltered from Chiniak Bay by the southern tip of Near Island but is exposed to occasional strong winds out of Womens Bay, which generate seas that are hazardous to small craft. The map of the area given in Figure 1, taken from the Alaska Coastal Data Collection Program Data (ACDCP) report, shows the locations of measurement devices and other features discussed in this report.
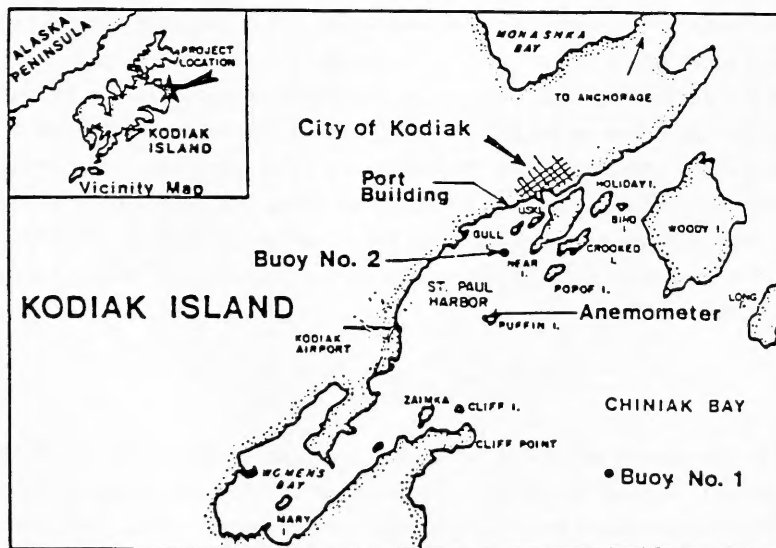

Figure 1.   Kodiak area map and data collection
and telemetry system

Hindcast Data Selection

5.   The hindcast wave data set used in this study was provided on mag-
netic tape by WIS. The data consisted of one record of wave climate charac-
teristics including significant wave height, period, and direction for every
3 hr for the years from 1956 to 1975 for a total of approximately 58,400 rec-
ords (Ragsdale 1983). A computer program was developed to search this tape
for records having specific directions and magnitudes. The program writes
tabular listings of the selected data records for further data reduction.
The WIS grid point (Point 17) that is nearest to the Chiniak Bay area is
120 nautical miles east of Kodiak (see Figure 2). Events producing signif-
icant wave heights of 6 m or more were chosen and maximum significant wave
height and associated period were then selected for each event. Appendix A
provides a listing of the 78 resulting maximum significant wave heights,
each with its date of occurrence and period. The choice of 6 m as a selec-
tion criterion was arbitrary. However, the choice was modified and vali-
dated in terms of the resulting extremal analysis. The data were surveyed
for significant storm events with wave directions corresponding to a direc-
tion window defined by Cape Chiniak to the south and Long Island to the north.
This window was taken to be approximately 95 to 140 degrees relative to True
North for waves traveling from the north and 90 degrees for waves from the
east. The direction window was constructed using the approximate center of
the St. Paul Harbor area (a little to the northwest of Puffin Island) as the
vertex of a triangle with the other two vertices defined by Cape Chiniak and
Long Island.

Probability Distribution for the
Number of Storms per Year

6.   The number of storms per year producing significant wave heights of
6 m or more is listed in Table 1. Note that for 1957 there was no event pro-
ducing significant wave heights of 6 m or more; whereas 1963, 1968, and 1969
each produced seven such events. The number of storms per year is listed with
its observed frequencies in Table 2. A common assumption for studies of this
type is that the number of storms per time interval is distributed according
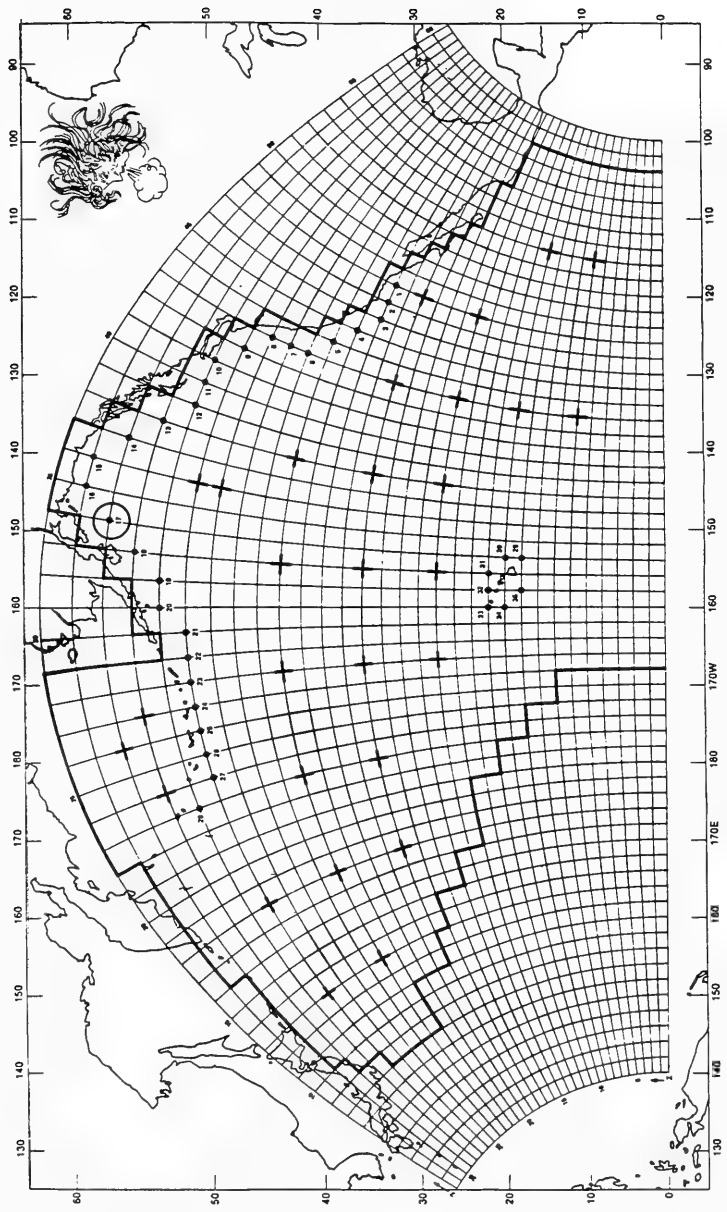
MERCATOR PROJECTION OF PACIFIC OCEAN

Figure 2. WIS hindcast grid points. Point 17 used for this study

7

Table 1

Annual Number of Storms Producing Significant

Wave Heights of 6 m or More

Year	Number of Storms
1956	1
1957	0
1958	5
1959	3
1960	5
1961	3
1962	5
1963	7
1964	4
1965	2
1966	3
1967	5
1968	7
1969	7
1970	3
1971	1
1972	5
1973	6
1974	3
1975	3
	78 = N

Table 2

Frequency Table for the Number of Storms per

1-Year Interval Producing Significant

Wave Heights of 6 m or More

Number of Storms	Frequency
0	1
1	2
2	1
3	6
4	1
5	5
6	1
7	3

8

to a Poisson probability distribution (Borgman and Resio 1982). The Poisson distribution has probability density

$$p(x) = \frac{u^x e^{-u}}{x!} \; , \; x = 0 \;,\; 1 \;,\; 2 \;,\; 3 \;,\; \ldots \tag{1}$$

The variable x is the number of storms per year and the parameter u is the average number of storms per year in this case, and $u = 78$ storms/20 years or $u = 3.9$.

    7. The chi square goodness of fit test is used to test the validity of the Poisson assumption (Miller and Freund 1977). The test is based on the statistic x_n^2

where

$$x_n^2 = \sum_{i=1}^{n} \frac{\left(O_i - E_i\right)^2}{E_i} \tag{2}$$

and

   O_i = observed frequency of years with $i - 1$ storms

   E_i = Poisson expected frequency of years with $i - 1$ storms

If x_n^2 is small when compared to theoretical chi square values, then the probability that the Poisson assumption is valid will be great. Table 3 lists the values for O_i and E_i and the resulting value for x_n^2

Table 3

Chi Square Test for the Poisson Model

Number of Storms	O_i		E_i		$\left(O_i - E_i\right)^2/E_i$
0	1	3	0.40	1.98	0.525
1	2		1.58		
2	1	7	3.08	7.08	0.001
3	6		4.00		
4	1	6	3.90	6.94	0.127
5	5		3.04		
6	1	4	1.98	3.08	0.275
7	3		1.10		
					$x_n^2 = 0.928$

Some of the cells have been combined in the test to minimize the impact of small cell counts on the resulting statistic. The theoretical chi square

9

values are found in The Handbook of Mathematical Functions (Abramowitz and Stegun 1972).

For a chi square with 5-degrees of freedom (n = 4)

$$Pr\left(x_4^2 \geq 0.711\right) = 0.95$$

$$Pr\left(x_4^2 \geq 1.064\right) = 0.90$$

and by means of linear interpolation

$$Pr\left(x_4^2 \geq 0.928\right) = 0.92$$

Since the computed statistic is small compared to 92 percent of all possible chi square values, it is concluded that the Poisson assumption is valid. This result will be instrumental in defining such quantities as return period and nonencounter probability in the following sections of this report.

Extremal Theory

8. There are several theoretical probability distributions that have been successfully used in the fitting and subsequent extrapolation of extreme wave conditions. These are the Extremal or Fisher-Tippett Type I distribution, the Lognormal distribution, the Log Extremal distribution, and the Weibull distribution. These distributions have cumulative probability functions as listed in Table 4.

Table 4

Extremal Models

Extremal Type I:

$$F(x) = \exp\left\{-\exp\left[\frac{-(x - \mu)}{\sigma}\right]\right\} \tag{3}$$

$$-\infty < x < \infty$$

(Continued)

10

Table 4 (Concluded)

Lognormal:

$$F(x) = \frac{1}{\sqrt{2\pi}} \int_0^x \frac{1}{\sigma h} \exp\left[-\frac{1}{2}\left(\frac{\ln h - \mu}{\sigma}\right)^2\right] dh \tag{4}$$

$$0 < x < \infty$$

Log Extremal:

$$F(x) = \exp\left[-\left(\frac{x-\mu}{\sigma}\right)\right] \tag{5}$$

$$0 < x < \infty$$

Weibull:

$$F(x) = 1.0 - \exp\left[-\left(\frac{x-\mu}{\sigma}\right)^C\right] \tag{6}$$

9. The theoretical cumulative probability function is fit to data by means of the plotting position formula. If the data sample given by x_1, $x_2,\ldots,\ x_n$ is ranked in ascending order denoted by $Y_{(1)} < Y_{(2)} <\ldots< Y_{(n)}$ where $Y_{(k)}$ is called the kth order statistic, then the plotting position formula

$$\hat{F}_k = \frac{k}{n+1} \tag{7}$$

represents the estimate of the data cumulative probability function. If this is set equal to the proposed theoretical cumulative probability function $F(x)$ from Table 4 then

$$\hat{F}_k = \frac{k}{n+1} = F\left[AY_{(k)} + B\right] \tag{8}$$

where A and B are scale and location parameters, respectively. The inverse of the function in Equation 8 is

$$F^{-1}\left(\hat{F}_k\right) = B \bullet Y_{(k)} + A \tag{9}$$

If the plot of $F^{-1}(k/n + 1)$ with $Y_{(k)}$ approximates a straight line with slope A and intercept B then the proposed theoretical distribution is accepted. Sometimes more than one of the possible distributions will yield a straight line fit. In this case, the better of these is usually that which best fits the upper tail of the function $\hat{F}_k$. However, some subjective judgment is required in such cases.

10. The quantity known as the return period, R, is defined to be the mean value of the random number of observations preceding and including the first exceedence of a specified wave threshold x. In terms of the cumulative probability function and the Poisson model parameter u

$$R = \frac{1}{u[1 - F(x)]} \tag{10}$$

Another useful measure is the nonencounter probability, $NE(x)$, or the probability that for a design life L the largest wave condition is less than or equal to x in value. For the Poisson model

$$NE(x) = \exp\left(\frac{-L}{R}\right) \tag{11}$$

Note that if $L = R$ then

$$NE(x) = 0.37$$

Thus the probability of encountering a condition larger than the R year return period condition in R years is 0.63. This demonstrates the misleading nature of the return period in that during R years, there is a 63 percent chance of encountering an R year extreme condition. Care should be taken when using return period as the only criterion for extremal prediction.

Extremal Plotting

11. A computer software package called EXPLOT was developed at the US Army Engineer Waterways Experiment Station (WES) on the Honeywell DPS1 system to plot the formula given in Equation 9. The plotting was performed for each

of the functions listed in Table 4. The Weibull distribution was computed for values of C = 1.0 and C = 2.0 from Equation 6. These values represent the general range of Weibull shape parameters that are applicable to wave conditions. Note that if C = 1.0 , the Weibull reduces to an exponential distribution and if C = 2.0 , the Rayleigh distribution (Petrauskas and Aagaard 1971). The slope and intercept from Equation 9 are estimated by computing the least squares linear regression line corresponding to Equation 9 (Issacson and Mackenzie 1981). For a listing of estimated values of A and B along with the corresponding parameter estimates for each specific function see Table 5:

Table 5

Estimated Parameters for the Hypothesized Extremal Models

Model	A	B	μ	σ
Extremal Type I	-6.804	0.981	6.936	1.019
Lognormal	-8.058	1.128	7.144	0.886
Log Extremal	-14.952	7.742	7.742	6.898
Weibull, C = 1.0	-4.615	0.745	6.195	1.342
Weibull, C = 2.0	-1.839	0.363	5.066	2.755

12. Appendix B contains the resulting data plots for each of the proposed extremal models. The horizontal axis entitled Cumulative Probability Scale denotes the actual values of the function $F(x)$ from Table 4 that correspond to the data values on the vertical axis. The other horizontal axis is the return period as defined in Equation 10. By inspection it is seen that the Lognormal model does not fit. The Weibull with C = 1.0 , or exponential, also displays significant curvature. The Log Extremal model shows less curvature, but the plot still deviates from linearity in the upper and lower tails of the distribution. The Extremal Type I and the Weibull with C = 2.0 (Rayleigh) both look fairly linear except for the lowest 16 points. Since the choice of 6 m for the data selection threshold was arbitrary, it is intuitively appealing to recompute the analysis without the lower 16 points. This results in a total of 62 storm events with maxima greater than or equal to 6.4 m and a revised Poisson parameter of u = 3.1 storms per year. The chi square goodness of fit test for the Poisson distribution of storms per year was recomputed with the reduced data set. The chi square value was $x_4^2 = 1.35$ and $\left(Pr \ x_4^2 \geq 1.35 \right) \approx 0.85$. The chi square statistic is still smaller than 85 percent of all possible chi square values; therefore, it is

13

concluded that the Poisson model still holds. The extremal plots for the re-
duced data sets are displayed in Figures 3 and 4. The Extremal Type I and the
Weibull C = 2.0 both appear to fit the largest 62 data points well. The Ex-
tremal Type I is the preferred model because (a) it appears to fit better in
the upper tail of the data, (b) it is one of the three possible extremal as-
ymptotes (Borgman and Resio 1982), of which the Weibull is not a member and,
therefore, has a better theoretical basis than does the Weibull, and (c) the
Extremal Type I is a two-parameter model whereas the Weibull has three param-
eters. The Weibull shape parameter C makes it possible to fit the distribu-
tion to data with a higher degree of accuracy than for two-parameter models.
This fact does not necessarily mean that extrapolations beyond the data extent
will be improved by the higher precision fit. The extrapolations could be
very unreliable if the Weibull were used when a simpler model was more appro-
priate. Results will be given for both models, but it is believed that the
Extremal Type I is qualitatively the better model. Table 6 contains the val-
ues of A and B and the resulting distribution parameters. The return
periods and associated significant wave heights were computed for both models
and are presented in Table 7.
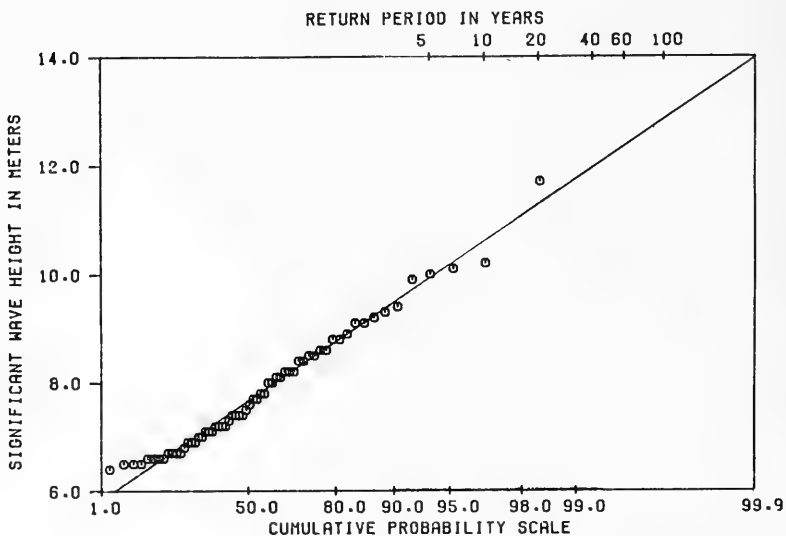
Figure 3. Extremal plot for 62 largest maximum
significant wave heights, Extremal Type I
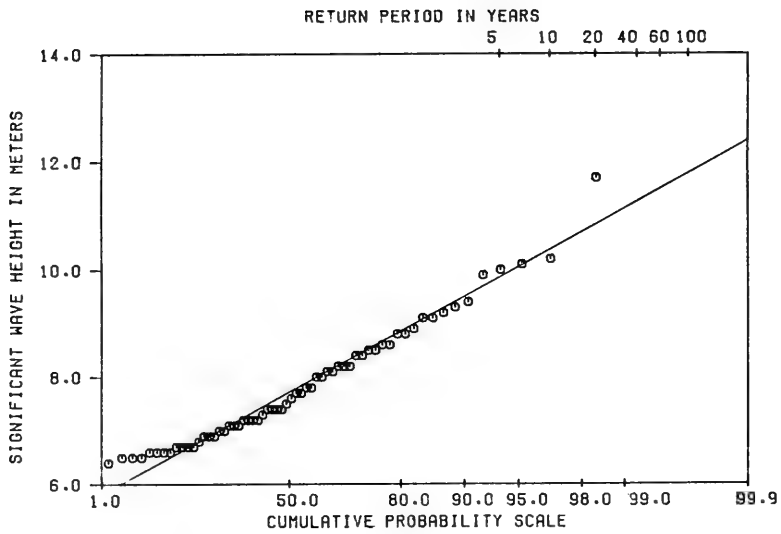
Figure 4. Extremal plot for 62 largest maximum
significant wave heights, Weibull, C = 2.0

Table 6

Estimated Parameters for the Selected Extremal Models

Model	A	B	μ	σ
Extremal Type I	-7.567	1.036	7.304	0.965
Weibull, C = 2.0	-2.130	0.384	5.547	2.604

Table 7

Predicted Significant Wave Heights and Associated

Return Periods for the Selected Models

Return Period years	Significant Wave Height, m
Extremal Type I	
5	9.92
10	10.60
20	11.28
40	11.95

(Continued)

15

Table 7 (Concluded)

Return Period years	Significant Wave Height, m
Extremal Type I (Continued)	
50	12.17
60	12.35
100	12.84
Weibull, C = 2.0	
5	9.86
10	10.37
20	10.84
40	11.26
50	11.39
60	11.50
100	11.78

13.   The concept that we refer to as "return period" has been shown to be prone to misinterpretation (Borgman 1963). The statement "50-year wave" may be taken to mean that waves of magnitude greater than or equal to the 50-year value occur on the average of once every 50 years. The phrase "on the average" is the key to interpreting this concept. As was seen in the discussion of nonencounter probabilities, the chance of encountering a 50-year wave in any given 50-year interval is about 63 percent. The nonencounter probabilities given in Table 8 are defined to be the probabilities for any given design life L that an R year wave is not encountered. These values can be used to give further meaning to the return periods and associated significant wave heights reported in Table 6.

Table 8

Estimated Nonencounter Probabilities

for the Extremal Type I Model

Design Life, years (L)	Return Period, years (R)				
	20	40	50	60	100
20	0.37	0.61	0.67	0.72	0.82
40	0.14	0.37	0.45	0.51	0.67
50	0.08	0.29	0.37	0.43	0.61
60	0.05	0.22	0.30	0.37	0.55
100	0.01	0.08	0.14	0.19	0.37

14.   Methods for computing the reliability of extreme wave condition estimates can be found in various reports and articles (Petrauskas and Aagaard 1971, Isaacson and Mackenzie 1981, Borgman 1983). The method given by Borgman requires relatively little computation while the other methods either do not apply to prediction or entail extensive numerical simulations. The method used here has been successfully applied to the extremal analysis of hindcast data on the coast of California (Borgman 1982).

15.   The first step in computing the estimate reliability is to calculate an upper bound on the error (standard deviation) σ_F from estimating the function $F(x)$ from Table 4. This upper bound is approximated by the Kolmogorov-Smirnov (KS) limit for the quantity

$$|\hat{F}_R - F(x)| \tag{12}$$

for $\hat{F}_R$ from Equation 7. The KS upper bound is the value $D(\alpha,n)$ such that

$$PR\left[\max|\hat{F}_R - F(x)| > D(\alpha,n)\right] = \alpha$$

for α = a small number. In other words, the number $D(\alpha,n)$ is such that the maximum absolute difference between the cumulative probability function $F(x)$ and its estimated value $\hat{F}_R$ will be greater than $D(\alpha,n)$ only with small probability α . The value $D(\alpha,n)$ is then assumed to represent a $Z_{\alpha/2} \times \sigma_F$ error where $Z_{\alpha/2}$ is the standard normal variate such that $Pr(Z < Z_{\alpha/2})$ = $\alpha/2$; thus, an approximate value for the error σ_F is computed to be

$$\alpha_F = \frac{D(\alpha,n)}{Z_{\alpha/2}} \tag{13}$$

For samples of $n > 35$ and $\alpha = 0.05$ an approximate value for $D(\alpha,n)$ given $n = 62$ is

$$D(0.05,n) = \frac{1.36}{\sqrt{62}}$$

and

$$Z_{0.025} = 1.96$$

then

$$\sigma_F = 0.09 \tag{14}$$

The value for σ_F represents the approximate sampling error or standard deviation involved in the estimation of $F(x)$. In order to state this error in terms of the Y-year significant wave height, it is necessary to define the quantity known as the coefficient of variation or CV . The CV is the standard deviation of a variable divided by the mean of the variable. At the median where $F(x) = 0.5$, the CV for the quantity $F(x)$ will be approximately

$$CV_F = \frac{\sigma_F}{0.5} \tag{15}$$

$$CV_F = 0.18 \tag{16}$$

The CV for $F(x)$ is approximately equal to the CV for $F_y(x)$, the cumulative probability density for the Y-year significant wave height (Borgman 1982); thus, if σ_{F_R} is the standard deviation for $F_y(x)$ and since $F_R(x)$ = 0.37 for the R-year wave, then

$$\sigma_{F_R} = 0.37CV_F$$

$$= 0.07 \tag{17}$$

16.   The final step in the reliability analysis is to express the error in terms of the R-year significant wave height error σ_{X_R} . This is accomplished by means of the approximate formula

$$\sigma_{X_R} = \frac{\sigma_{X_R}}{\partial_R} \tag{18}$$

where ∂_R = the slope of F_R evaluated at X_R . The formula for ∂_R is

$$\partial_R = uR \frac{\partial F(X_R)}{\partial x} \exp\left\{uR[1 - F(X_R)]\right\} \tag{19}$$

18

for u = the Poisson parameter or the mean number of storm events per year. The slope ∂_R for the Extremal Type I is approximately

$$\partial_R = 1.03 \qquad (20)$$

for all values of R from 20 to 100.

17. The error due to the hindcast model can also be included in the reliability analysis. The WIS hindcast model when compared to measured data shows at most a difference of about 0.04 for percent occurrence of significant wave heights larger than 6 m (Figure 11, Corson and Resio 1981). If this value is assumed to be the error in estimating $F(x)$ due to the hindcast model then σ_F from Equation 14 becomes

$$\sigma_F = 0.09 + 0.04 = 0.13 \qquad (21)$$

Recomputing Equations 15 through 17, the result is

$$\sigma_{F_R} = 0.10 \qquad (22)$$

and then by Equation 18 for the Extremal Type I

$$\sigma_{X_R} \cong 0.10 \qquad (23)$$

18. The error in the extremal prediction to a very rough approximation is about one-tenth of a meter. It is not yet known how accurate this error estimation technique is, and its results should be used with some subjective consideration.

Wave Period Distribution

19. The joint probability distribution for significant wave height versus period is listed in Table 9. For the extreme wave condition, the periods tend to be larger than 12 sec with periods at 14.3 sec for the three most extreme conditions in the 20-year period. This tendency suggests the use of a period of near 14.3 sec for the computation of design conditions.

Table 9

<u>Joint Frequency Distribution of Wave Period</u>

<u>Versus Significant Wave Height</u>

Significant Wave Height m	Wave Period, sec				
	11-	11-12	12-13	13-14	14-15
6 ≤ Hs < 7	6	14	9	0	3
7 ≤ Hs < 8	4	9	2	↓	5
8 ≤ Hs < 9	0	4	8		4
9 ≤ Hs < 10	0	0	5		1
10 ≤ Hs < 11	0	0	1		2
11 ≤ Hs < 12	0	0	0		1

PART III: ANALYSIS OF MEASURED WAVE DATA

Data Description

20. Data were provided to WES by US Army Engineer District, Alaska
(NPA), on magnetic tape duplicating that published in Data Reports 1 and 2 of
the ACDCP. These data consisted of three sets of tables: "Summary Table for
Wind/Wave Data," "Summary Table for Wind Data," and Energy Spectrum" tables
presenting data collected by two Waverider buoys. The Waverider buoys, de-
noted as buoy 1 (outer buoy) and buoy 2 (inner buoy), are located in Chiniak
Bay and St. Paul Harbor, and are in 77 m and 16 m of water, respectively (see
Figure 1). The data provided included measurements taken from October 1981
through September 1983. Also provided on magnetic tape was an edited version
of National Weather Service (NWS) anemometer data from 1945 through 1982 mea-
sured by an instrument located between the Kodiak Airport and Womens Bay at
the present site of the US Coast Guard Kodiak Air Station. The detailed for-
mat of the original data and modifications made during the analysis will be
described in the following paragraphs.

Data Selection

21. Extreme wave conditions for the north Pacific tend to occur dur-
ing the winter months. This is exemplified by the frequency distribution
for months with extreme wave conditions producing significant wave heights
of 6 m or more given in Table 10. The values in Table 10 were computed using
the hindcast data.

Table 10

Frequency Distribution of Months During Which Extreme

Events Occurred for the 20-Year Hindcast Period

Month	Frequency
October	9
November	17
December	20
January	22
February	7
March	2
April	1

22. The winter "storm season" is defined to be the months from October through April. With this definition, it is possible to consider only those months that would be expected to produce extremes in the measured data. This eliminates possible biases due to the mixture of monthly maxima resulting from storms with those resulting from regular conditions.

Extremal Plotting of Monthly Maxima

23. The monthly maxima were fit to the Weibull probability model with shape parameter $C = 1$, and $C = 2$ and to the Extremal Type I. As for the hindcast data, the Extremal Type I displays a better fit than does the Weibull. Figures 5 through 10 represent the extremal plots for the measured data. The extreme wave conditions and associated return periods given in Table 11 were computed from the fitted Extremal Type I model. The values

Table 11

Significant Wave Height and Return

Period for Measured Data

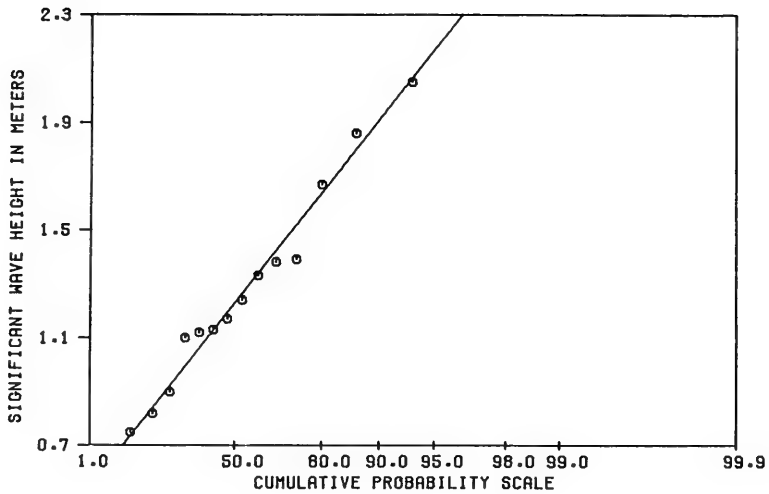| Return Period years		Significant Wave Height m
	Inner Buoy	
1		1.8
2		2.0
3		2.2
4		2.3
5		2.4
10		2.6
50		3.2
100		3.5
	Outer Buoy	
1		4.5
2		5.4
3		5.9
4		6.3
5		6.5
10		7.4
50		9.3
100		10.1

Figure 5. Extremal plot for monthly maximum signifi-
cant wave heights measured at the Inner Buoy location,
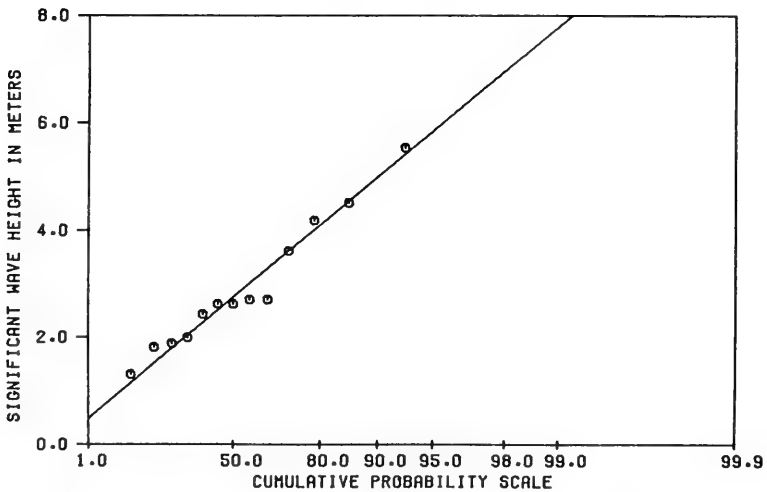Extremal Type I

Figure 6. Extremal plot for monthly maximum signifi-
cant wave heights measured at the Outer Buoy location,
Extremal Type I

23

Figure 7. Extremal plot for monthly maximum signifi-
cant wave heights measured at the Inner Buoy location,
Weibull C = 2.0

Figure 8. Extremal plot for monthly maximum signifi-
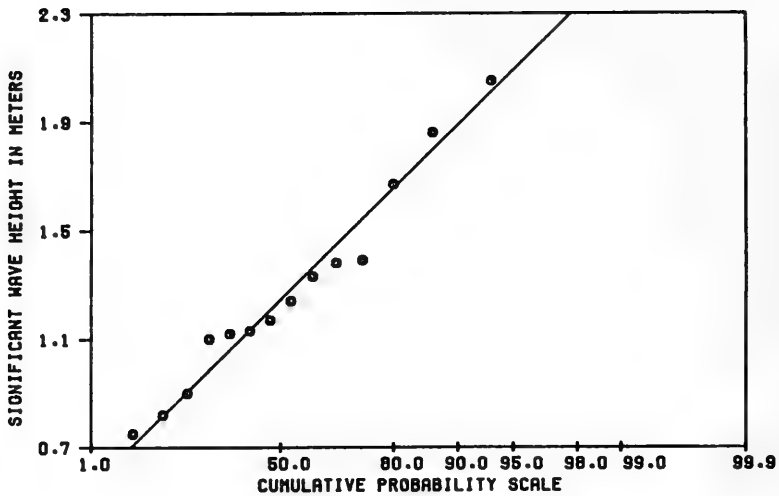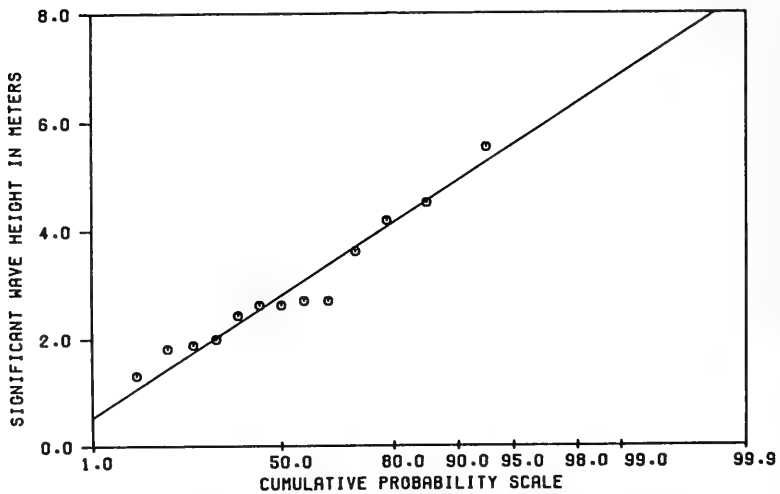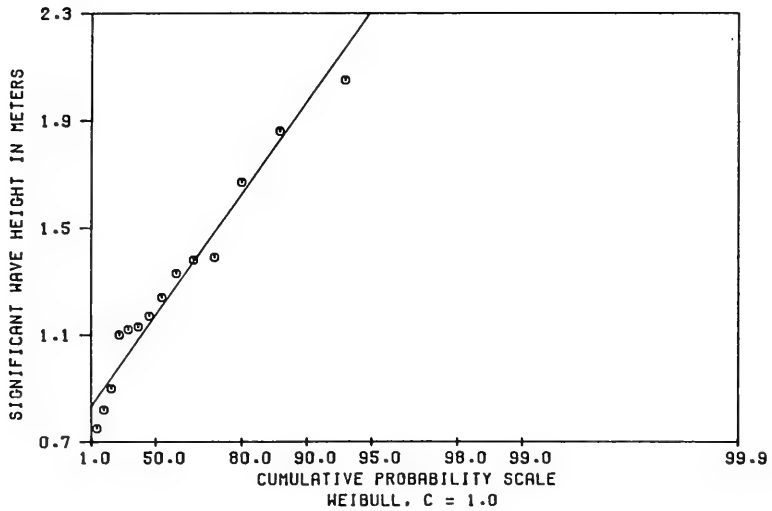cant wave heights measured at the Outer Buoy location,
Weibull C = 2.0

Figure 9. Extremal plot for monthly maximum signifi-
cant wave heights measured at the Inner Buoy location,
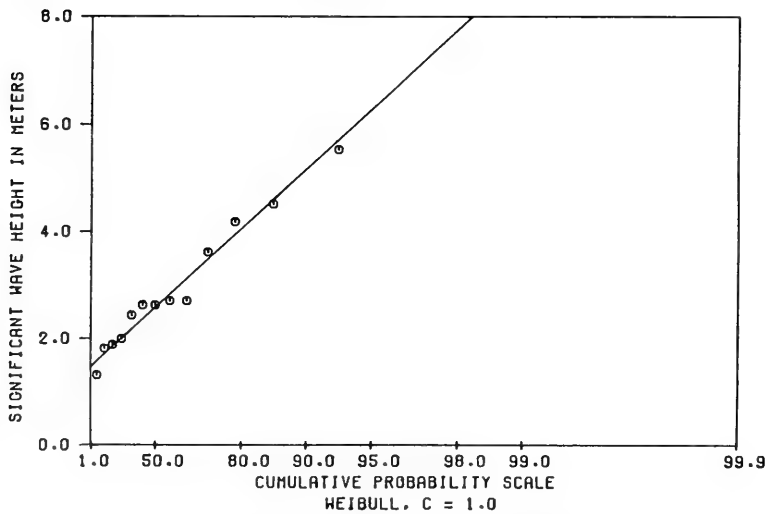Weibull C = 1.0

Figure 10. Extremal plot for monthly maximum signifi-
cant wave heights measured at the Outer Buoy location,
Weibull C = 1.0

given in Table 11 are intended for comparison with the hindcast values but not for use in constructing long-term extreme wave conditions. It is a generally accepted rule of thumb that any extrapolation beyond twice the extent of the data becomes highly unreliable (Borgman and Resio 1982); hence, 2 years of data may be useful for predicting 2 to 5 years of wave conditions but are not very reliable for 5- to 100-year predictions.

Discussion

24. The use of measured data to make long-term wave condition estimates has been discussed in several recent articles (Carter and Challenor 1978, Challenor 1982, and Wang and LeMehaute 1983). The key aspect of the theory of extremes is that in looking at enough years of data, the chance of seeing most types of hazardous events is good. In this respect, measured data will become useful as longer records are made available. At this time, hindcast data fulfill the need. The wave data that were measured at Kodiak provide an interesting comparison to hindcast results.

25. It is surprising that the outer buoy, or buoy 1, did not display at least one maximum significant wave height in exceedance of 6 m. If it is assumed that the hindcast grid point represents the same general wave condition as the outer buoy, and since there were 78 events producing significant wave heights of 6 m or more in the 20-year hindcast time period, the probability of seeing two consecutive years with no significant wave heights greater than 6 m at the outer buoy is nearly zero. Because of this, it is not possible to either support or contradict the results from the hindcast analysis using the measured wave data. If consecutive hindcast and measured values were available, this behavior could be studied; however, such is not the case at this time.

Analytical Procedures

26. Two FORTRAN computer programs provided the principal tools for
analysis of the data measured at Kodiak: "Statistical Package for the Social
Sciences" (SPSS) and a program titled "WINSUM." SPSS is a comprehensive soft-
ware system of advanced statistical routines, originally developed by the
National Opinion Research Center of the University of Chicago. SPSS statisti-
cal routines are highly versatile and applicable to most scientific and engi-
neering data. WINSUM was developed by the Coastal Engineering Research Center
for analysis of periodic wind measurements. These two programs and a number
of supportive editing and plotting routines were executed on the WES Honeywell
DPS-1 system.

27. Data from the "Summary Tables for Wind/Wave Data" and the "Summary
Tables for Wind Data" were first reduced to a simple listing of consecutive
individual readings in a predetermined FORTRAN format. Individual runs of
SPSS accomplished additional grouping value corrections, accounting of missing
values, and labeling required by particular statistical procedures. Zero val-
ues were included with missing values. Similarly, the NWS wind data were re-
duced to a simple listing of consecutive readings in a format compatible with
WINSUM and correlations related to the physical characteristics of the mea-
surement site were also accomplished.

Wave Data Analysis

28. The "Summary Table for Wind/Wave Data" presents the significant
(zero-moment) wave heights and peak periods for each sample from both wave
buoys. A description of how these values were computed from the original time
series data is provided by the ACDCP (1983a, b). The complete record was ana-
lyzed for the frequency distribution of wave heights in classes of 2 ft each
and of peak periods in classes of 2 sec each. The results of this procedure
are presented in Tables 12-15.

29. Dependence of conditions measured at the inner buoy on conditions
measured concurrently at the outer buoy were first tested by SPSS scattergram
routines which included simple linear regression. These measurements were

27

Table 12

Frequency Distribution Analysis for the Outer Buoy

Location Significant Wave Height Measurements

Category Label	Code	Absolute	Frequency Relative percent	Adjusted percent	Cumulative percent
Less than 2 ft	1	1,889	36.3	52.8	52.8
2 to 4 ft	2	1,054	20.3	29.5	82.3
4 to 6 ft	3	378	7.3	10.6	92.8
6 to 8 ft	4	147	2.8	4.1	97.0
8 to 10 ft	5	60	1.2	1.7	98.6
10 to 12 ft	6	29	0.6	0.8	99.4
12 to 14 ft	7	17	0.3	0.5	99.9
14 to 16 ft	8	1	0.0	0.0	99.9
Over 16 ft	9	2	0.0	0.1	100.0
	-1	1,625	31.2	Missing	100.0
	Total	5,202	100.0	100.0	

Mean	1.772	Standard error	0.018	Median	1.447
Mode	1.000	Standard deviation	1.088	Variance	1.183
Kurtosis	5.108	Skewness	1.978	Range	8.000
Minimum	1.000	Maximum	9.000		

Valid cases   3,577
Missing cases 1,625

Table 13

Frequency Distribution Analysis for the Inner Buoy

Location Significant Wave Height Measurements

Category Label	Code	Frequency Absolute	Relative percent	Adjusted percent	Cumulative percent
Less than 2 ft	1	4,062	78.1	83.1	83.1
2 to 4 ft	2	765	14.7	15.6	98.7
4 to 6 ft	3	62	1.2	1.3	100.0
6 to 8 ft	4	2	0.0	0.0	100.0
	-1	311	6.0	Missing	100.0
	Total	5,202	100.0	100.0	

Mean	1.183	Standard error	0.006	Median	1.102
Mode	1.000	Standard deviation	0.421	Variance	0.177
Kurtosis	4.459	Skewness	2.215	Range	3.000
Minimum	1.000	Maximum	4.000		

Valid cases   4,891
Missing cases   311

Table 14

Frequency Distribution Analysis for the Outer Buoy
Location Peak Period Measurements

Category Label	Code	Absolute	Frequency Relative percent	Adjusted percent	Cumulative percent
Less than 2 sec	1	14	0.3	0.4	0.4
2 to 4 sec	2	373	7.2	10.4	10.8
4 to 6 sec	3	454	8.7	12.7	23.5
6 to 8 sec	4	736	14.1	20.6	44.1
8 to 10 sec	5	1,161	22.3	32.5	76.5
10 to 12 sec	6	379	7.3	10.6	87.1
12 to 14 sec	7	210	4.0	5.9	93.0
Over 14 sec	8	250	4.8	7.0	100.0
	-1	1,625	31.2	Missing	100.0
	Total	5,202	100.0	100.0	

Mean	4.645	Standard error	0.027	Median	4.682
Mode	5.000	Standard deviation	1.600	Variance	2.559
Kurtosis	-0.284	Skewness	0.231	Range	7.000
Minimum	1.000	Maximum	8.000		

Valid cases   3,577
Missing cases   1,625

Table 15

Frequency Distribution Analysis for the Inner Buoy

Location Peak Period Measurements

Category Label	Code	Frequency Absolute	Relative percent	Adjusted percent	Cumulative percent
Less than 2 sec	1	79	1.5	1.6	1.6
2 to 4 sec	2	615	11.8	12.6	14.2
4 to 6 sec	3	782	15.0	16.0	30.2
6 to 8 sec	4	1,112	21.4	22.7	52.9
8 to 10 sec	5	1,223	23.5	25.0	77.9
10 to 12 sec	6	404	7.8	8.3	86.2
12 to 14 sec	7	206	4.0	4.2	90.4
Over 14 sec	8	470	9.0	9.6	100.0
	-1	311	6.0	Missing	100.0
	Total	5,202	100.0	100.0	

Mean	4.466	Standard error	0.025	Median	4.372
Mode	5.000	Standard deviation	1.757	Variance	3.089
Kurtosis	-0.386	Skewness	0.401	Range	7.000
Minimum	1.000	Maximum	8.000		

Valid cases   4,891
Missing cases   311

taken for approximately 20 min at the outer buoy immediately followed by a similar sample of the inner buoy. This sequence and the time lapse involved is effectively the same as concurrent measurement, since conditions at sea, particularly more extreme conditions, very rarely change that fast. The scattergram of HS2 (inner buoy significant wave height) and HS1 (outer buoy) shows some linearity, as indicated in Figure 11 (R^2 = 0.39). TP2 (inner buoy peak period) and TP1 (outer buoy) do not show any statistical relation, though visually the scattergram (Figure 12) indicates TP2 tends to equal TP1 in many cases. Attempts to run scattergrams of $HS2^2$ with $HS1^2$ and $HS2/gTP2^2$ with $HS1/gTP1^2$ produced no meaningful information. The significant wave heights were originally computed as representative of energy in the sea state, so the relation of energy levels is inherent in any comparison of HS2 with HS1. Squaring these values apparently only exaggerated the scatter. H/gT^2, as a measure of wave steepness, showed no statistical trends apparently because the peak periods by themselves didn't either.

30. Attempts to relate measured wave conditions to concurrently measured wind direction did not yield any dramatic conclusions, but they did reinforce the intuitive assumption that the most severe wave conditions exist with winds from Chiniak Bay. Figure 13 is a scattergram of HS2 with DIR (direction), in which cases with HS1 < 1.0 m and TP1 < 4.0 sec were excluded. The grouping of lower HS2 values in the range 280-360 deg indicates the relative frequency of offshore winds. HS2 values above 1 m are grouped in the range 45-180 deg. Figure 14 is a scattergram of HS1 with DIR, showing similar indications. The ratio TP2/TP1 plotted against DIR in Figure 15 shows the tendency for TP2 to equal TP1 with directional grouping similar to the wave height scattergrams. Womens Bay winds blow toward Puffin Island in the 200- to 250-deg range. This range has few points plotted on the three scattergrams, indicating severe wave conditions concurrent with winds from Womens Bay are rare.

31. SPSS procedures attempting to correlate wind velocity at Puffin Island with significant wave heights did not reveal any meaningful conclusions. The relationship of wind velocity to significant wave height is known to be highly nonlinear, however, and includes a number of other equally critical independent variables. Wind velocity data are, therefore, treated separately in this report with a view toward application of these nonlinear relationships.

FILE NONAME   (CREATION DATE = 04/13/84)
SCATTERGRAM OF (DOWN) HS2   SIG WAVE HT 2   (ACROSS) HS1   SIG WAVE HT 1

Figure 11. Scattergram for significant wave height at the Outer
Buoy (HS1) versus significant wave height at the Inner Buoy

33

FILE NONAME (CREATION DATE = 04/13/84)
SCATTERGRAM OF (DOWN) TP2 PEAK PERIOD 2
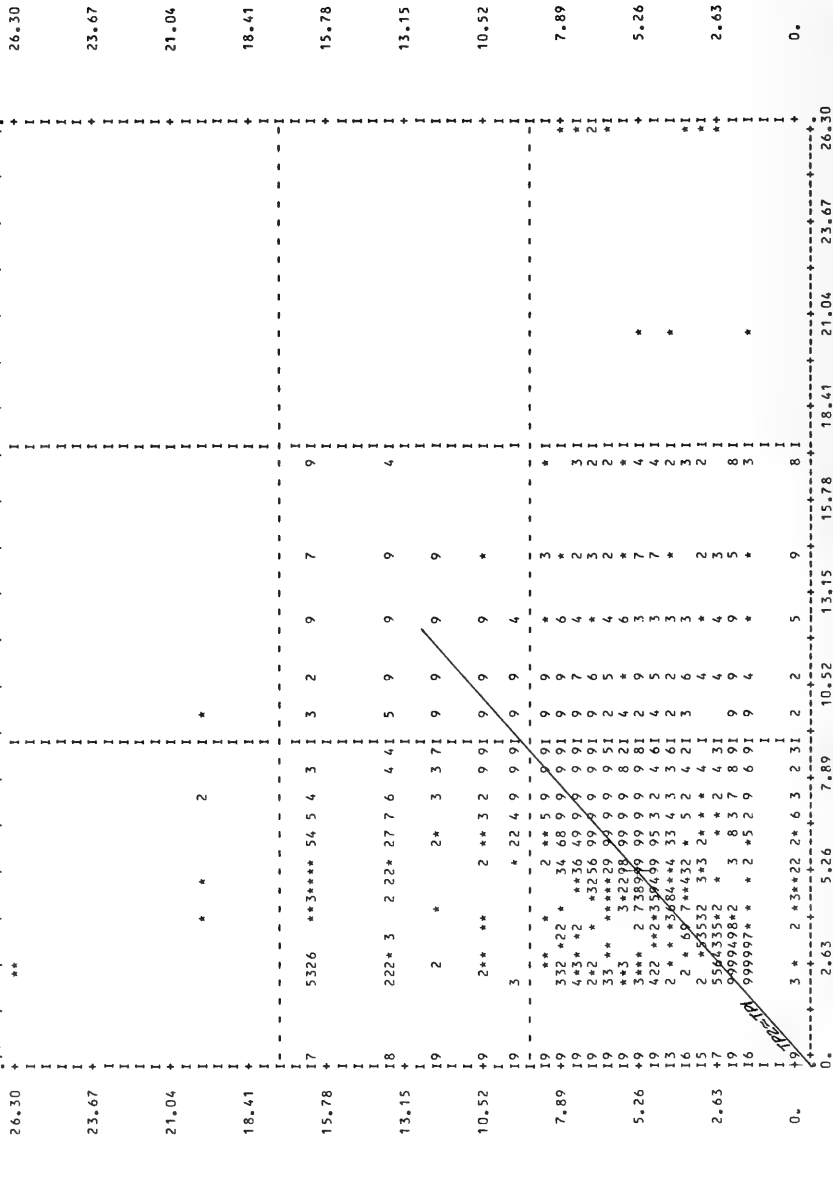
PEAK PERIOD 1
(ACROSS) TP1

Figure 12. Scattergram of peak period at the Outer Buoy (TP1)
versus peak period at the Inner Buoy (TP2)

FILE   NONAME   (CREATION DATE = 04/13/84)
SCATTERGRAM OF   (DOWN) HS2   SIG WAVE HT 2   (ACROSS) DIR
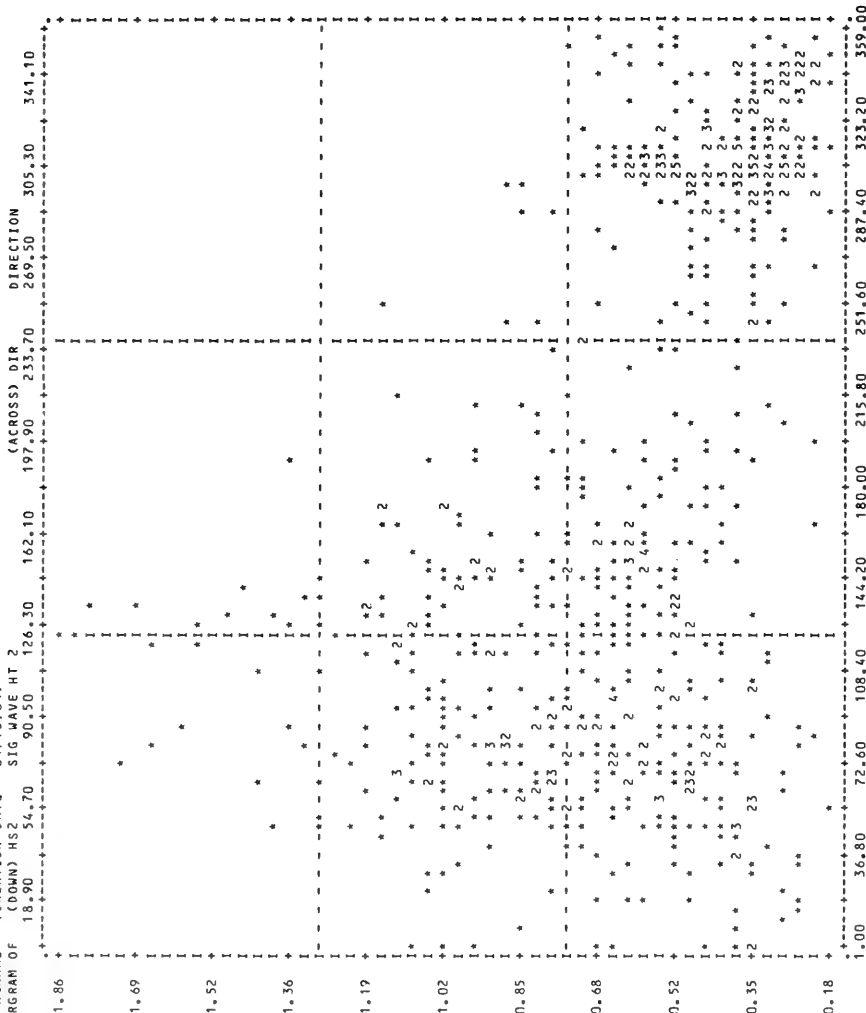
Figure 13.   Scattergram of significant wave height at the
             Inner Buoy (HS2) versus wind direction (DIR)

KODIAK WAVE DATA ANALYSIS   04/13/84   PAGE   5

FILE NONAME   (CREATION DATE = 04/13/84)
SCATTERGRAM OF (DOWN) HS1   SIG WAVE HT 1   (ACROSS) DIR

This page consists of a computer-printed scattergram (SIG WAVE HT 1 on the vertical axis, DIR on the horizontal axis) plotting significant wave height versus wind direction. The vertical axis is labeled with values from 5.53 down to 1.01, and the horizontal axis is labeled with direction values.

Vertical axis labels (left and right): 5.53, 5.08, 4.63, 4.17, 3.72, 3.27, 2.82, 2.37, 1.91, 1.46, 1.01

Horizontal axis (DOWN) HS1 values: 18.90, 54.70, 90.50, 126.30, 162.10, 197.90, 233.70, 269.50, 305.30, 341.10

DIRECTION axis (top): 18.90 54.70 90.50 126.30 162.10 197.90 233.70 269.50 305.30 341.10

Bottom axis: 1.00 36.80 72.60 108.40 144.20 180.00 215.80 251.60 287.40 323.20 359.00

Figure 14. Scattergram of significant wave height at the
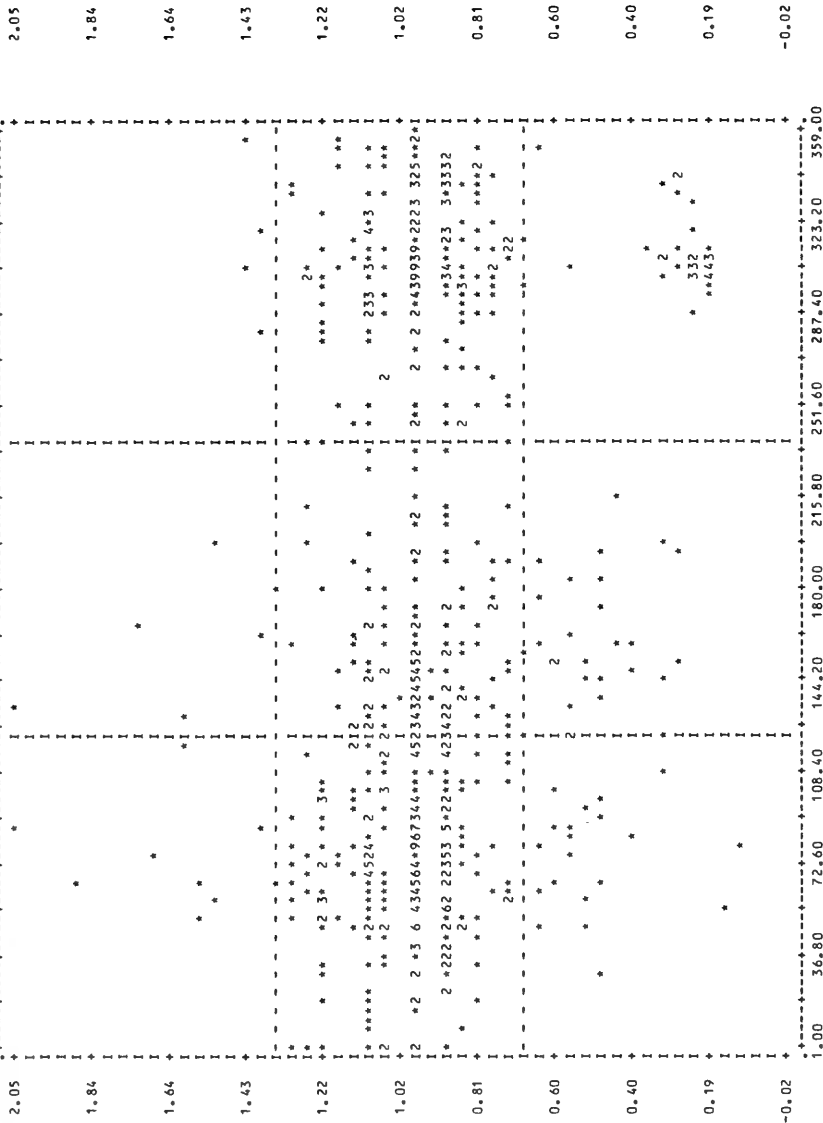   Outer Buoy (HS1) versus wind direction (DIR)

Figure 15. Scattergram of the ratio of peak period at the Inner Buoy (TP2) over peak period at the Outer Buoy (TP1) versus wind direction

37

32. The most significant statistical relationship, following prelimi-
nary analyses, appeared to be the reduction of significant wave height between
buoy 1 and buoy 2, as revealed by the scattergrams. SPSS procedures, which
computed multiple stepwise regression of HS2 with factors including HS1, $HS1^2$,
$HS1^3$, TP1, and $TP1^2$ were executed. Table 16 is a summary of a run where cases
with TP1 < 4 sec were excluded. The independent variables are listed in
order of their relative significance in the regression equation:

$$Y = A + B_1X_1 + B_2X_2 + \ldots + B_nX_n \tag{24}$$

where A and B_n are constants and X_n is the independent variable. The
changes in the correlation (R^2) indicate that HS1 provides the only important
correlation, with TP1 as next most important though comparatively insignifi-
cant. Nonlinear correlations were not revealed by inclusion of the $HS1^2$,
$HS1^3$, or $TP1^2$ terms.

Table 16

Regression Summary for the Multiple Linear Regression of HS2
with HS1, $HS1^2$, $HS1^3$, TP1, and $TP1^2$ for TP1 $\geq$ 4 sec

Variable	Multiple R	R Square	RSQ Change	Simple R	B	Beta
HS1 - Sig Wave Ht 1	0.74649	0.55725	0.55725	0.74649	0.44623	1.11870
TP1 - Peak Period 1	0.76011	0.56266	0.00542	-0.02561	-0.02978	-0.30323
TP1SQ - TPeak1 Squared	0.75218	0.56578	0.00312	-0.05501	0.00108	0.24627
HS1SQ - HSIG1 Squared	0.75358	0.56788	0.00209	0.67612	-0.07965	-0.66127
HS1CU - HSIG1 Cubed	0.75513	0.57022	0.00235	0.56785	0.01090	0.33109
(Constant)					0.26593	

33. Scattergrams of HS2 with HS1 which excluded cases with TP1 values
below an increasing lower limit showed increasing correlation. Figure 16 is
a scattergram of HS2 with HS1 where cases with TPA < 12 sec were excluded.
The R^2 computed was 0.73 with 405 cases included. The grouping near axes
intersection and along the HS2 = HS1 line is typical of all the scatter-
grams where only lower TP1 values were excluded. Figure 17 is a scattergram
of HS2 with HS1 where the following conditions were specified: TP1 $\geq$ 12 sec ,
HS2 $\geq$ 0.5 m , and HS1 $\geq$ 1.5 m . The R^2 computed was 0.75 with 38 cases
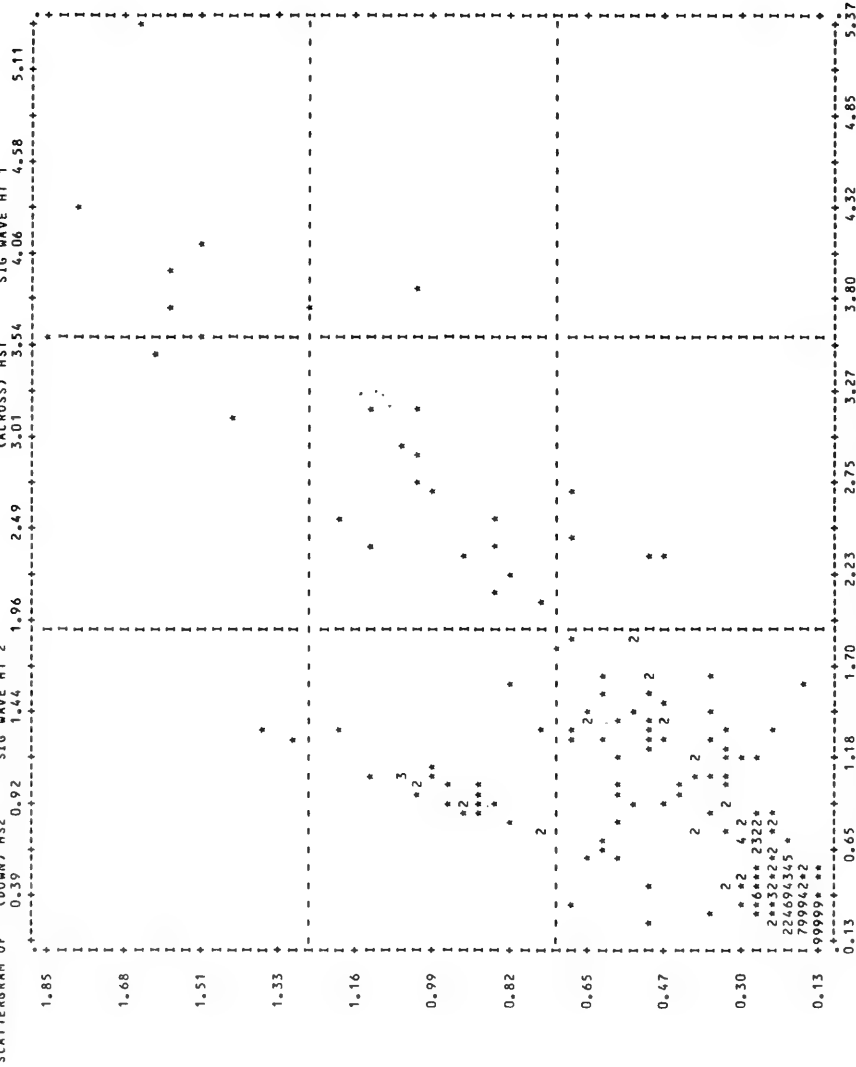
Figure 16. Scattergram of significant wave height at the Outer Buoy (HS1) versus significant wave height at the Inner Buoy (HS2) for peak periods ≥ 12 sec

39

KODIAK WAVE DATA ANALYSIS

04/30/84   PAGE 4

FILE   NONAME   (CREATION DATE = 04/30/84)
SCATTERGRAM OF   (DOWN) HS2   SIG WAVE HT 2   (ACROSS) HS1   SIG WAVE HT 1

Across (SIG WAVE HT 1): 2.12   2.51   2.89   3.27   3.65   4.03   4.42   4.80   5.18
                        1.74   1.93   2.31   2.70   3.08   3.46   3.84   4.22   4.61   4.99   5.37

Down (HS2 / SIG WAVE HT 2): 1.85   1.72   1.58   1.45   1.31   1.18   1.05   0.91   0.78   0.64   0.51
                            1.85   1.72   1.58   1.45   1.31   1.18   1.05   0.91   0.78   0.64   0.51   1.55

Figure 17.   Scattergram of significant wave height at the Outer Buoy (HS1) versus significant wave height at the Inner Buoy (HS2) for peak periods $\geq$ 12 sec and HS1 $\geq$ 1.5 m, HS2 $\geq$ 0.5 m

included. The complete regression statistics for this condition are presented
in Table 17. The linear regression equation resulting from this analysis is:

$$HS2 = 0.003 + 0.374 \ HS1 \qquad (25)$$

The intercept is notably very near zero indicating that an attenuation factor
of 0.37 for the conditions stated above has significance. In fact the 90 per-
cent confidence interval on the intercept, given by (-0.17, 0.18), contains
zero indicating that the intercept is not significantly different from zero
in a statistical sense. The slope or attenuation factor has 90 percent con-
fidence interval (0.31, 0.43).

Table 17

Linear Regression Summary for Inner Buoy

Significant Wave Height (HS2) and Outer

Buoy Significant Wave Height (HS1)

Variable(s) Entered on Step Number 1

Multiple R	0.86888
R Square	0.75495
Adjusted R Square	0.74814
Standard Error	0.19925

Analysis of Variance	DF	Sum of Squares	Mean Square	F
Regression	1	4.40304	4.40304	110.90697
Residual	36	1.42921	0.03970	

Variables in the Equation

Variable	B	Beta	Standard Error B	F
HS1	0.37425	0.86888	0.03554	110.907
(Constant)	0.00311			

41

PART V: ANALYSIS OF MEASURED WIND DATA

NWS Data

34. The NWS anemometer is located at the Coast Guard Station within Womens Bay. The anemometer is approximately 100 yd from the water line at mean sea level, elevation 10 m. Prior to 1973, a Navy anemometer was at the same location, but at an elevation of 5 m. The NWS/Navy anemometer provided hourly data from November 1945 through December 1982.

Data adjustment

35. Using the method presented in the Coastal Engineering Technical Note CETN-I-5, "Method of Determining Adjusted Windspeed, U_a , for Wave Forecasting," WES personnel adjusted the data. The adjustments included the following:

    a. Correction to 10-m level for data prior to 1973.

    b. Correction to hourly averages from 5-min averages every hour.

    c. Adjustment of overland readings to overwater readings.

    d. Correction for nonconstant coefficient of drag.

    e. Correction for instability due to air-sea temperature differences for directions where the fetch is greater than 10 miles (an unstable condition was assumed, since no temperature data were available).

These corrections were made so that the wind data could be applied directly to wave forecasting curves.

Wind summary

36. A computer program was developed to produce summaries of the hourly winds and of the 3-, 6-, 8-, and 10-hourly winds. The summaries relate wind speed and duration to recurrence probability for 16 directional sectors. The maximum annual wind was also found for use in an extremal analysis to be presented later.

37. The procedure to compute the N-hour average wind was as follows:

    a. Delete bad observations (less than 1 percent of the 325,050 observations were bad).

    b. Compute arithmetic average of all wind speeds in consecutive N-hour intervals to estimate wind speed (calm values were counted as zero wind speeds).

    c. Compute vector sum of all noncalm observations in the N-hour interval.

         <u>d</u>.   Compute direction of vector sum from <u>c</u> to estimate wind
            direction.

    38. The distribution of the hourly winds with respect to direction is
shown as a wind rose (Figure 18). The wind rose shows the distribution of
winds in 16 directional sectors as a percent of all winds. The bars in each
direction are broken into 10-mph intervals.

    39. The distributions of wind speed and duration relating to return
period are presented in Figure 19. Figure 19 shows combined data from all
sectors (0-360 deg). The curves represent the visual best fit to the data.
From these curves, the wind speed for a given return period can be obtained.
In general, these curves should not be extrapolated beyond twice the period
of record (37 years).

<center>Puffin Island Data</center>

    40. The Puffin Island anemometer is part of the ACDCP. Puffin Island
is located 1.5 miles offshore in Chiniak Bay. The anemometer is located at an
elevation of 23 m (island elevation) plus 6.1 m (elevation of sensor above the
island). The anemometer supplied about 16 months of usable data starting late
in 1981. The anemometer was not working in October and November of 1981 nor
in October of 1982, months when major storms are expected. The anemometer was
also out during other extreme events, so the data for extreme events are un-
reliable. The observations were 1-hr averages at 3-hr intervals.

<u>Data adjustments</u>

    41. Again, the raw data were adjusted using the method presented in
CETN-I-5. The adjustments included:

         <u>a</u>. Correction to 10-m level.

         <u>b</u>. Adjustment of overland readings to overwater readings.

         <u>c</u>   Correction for nonconstant coefficient of drag.

         <u>d</u>. Correction for instability due to air-sea temperature differ-
            ences for directions where the fetch is greater than 10 miles
            (an unstable condition was assumed, since no temperature data
            were available).

A calibration correction factor of 1.06 was also applied as recommended by the
Alaska District. An additional adjustment was made to account for the influ-
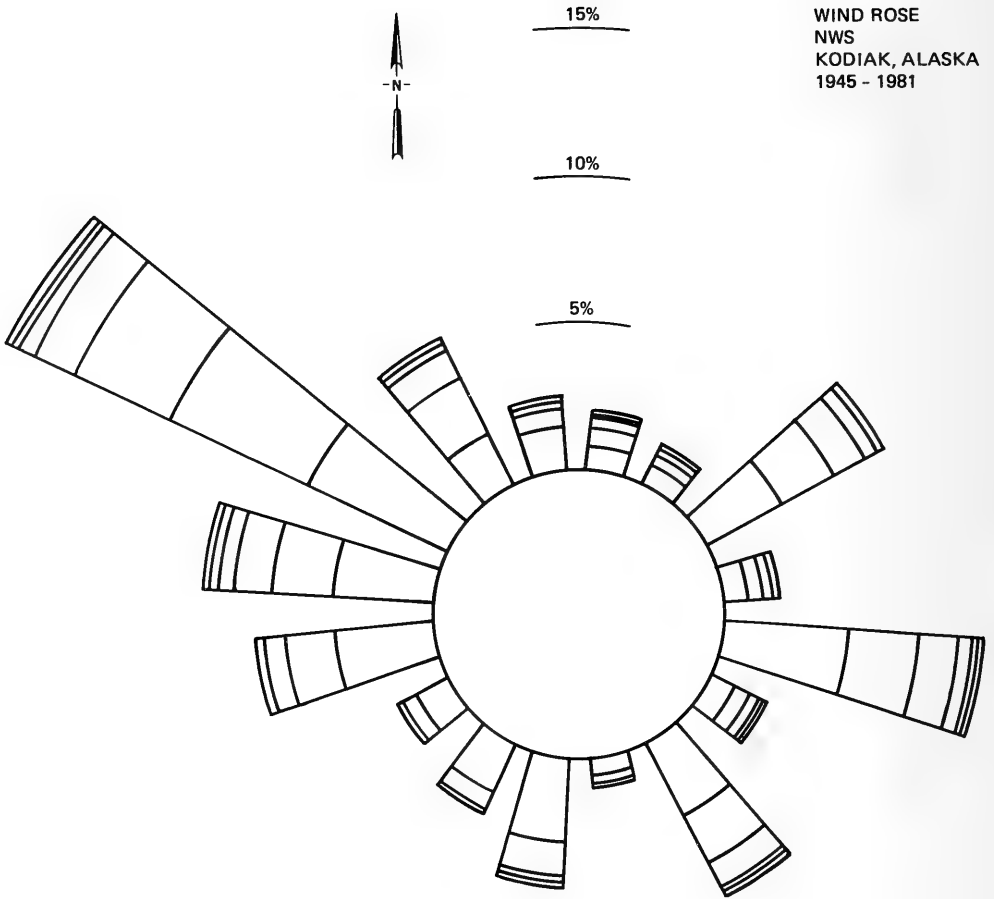ence of the island height and shape on the airflow (Simiu and Scanlon 1978).

15%

10%

5%

WIND ROSE
NWS
KODIAK, ALASKA
1945 - 1981

-N-

Figure 18. Wind rose for NWS data

44

NWS – ALL SECTORS

LEGEND
□ 1-HR DURATION
○ 3-HR DURATION
▲ 6-HR DURATION
■ 8-HR DURATION
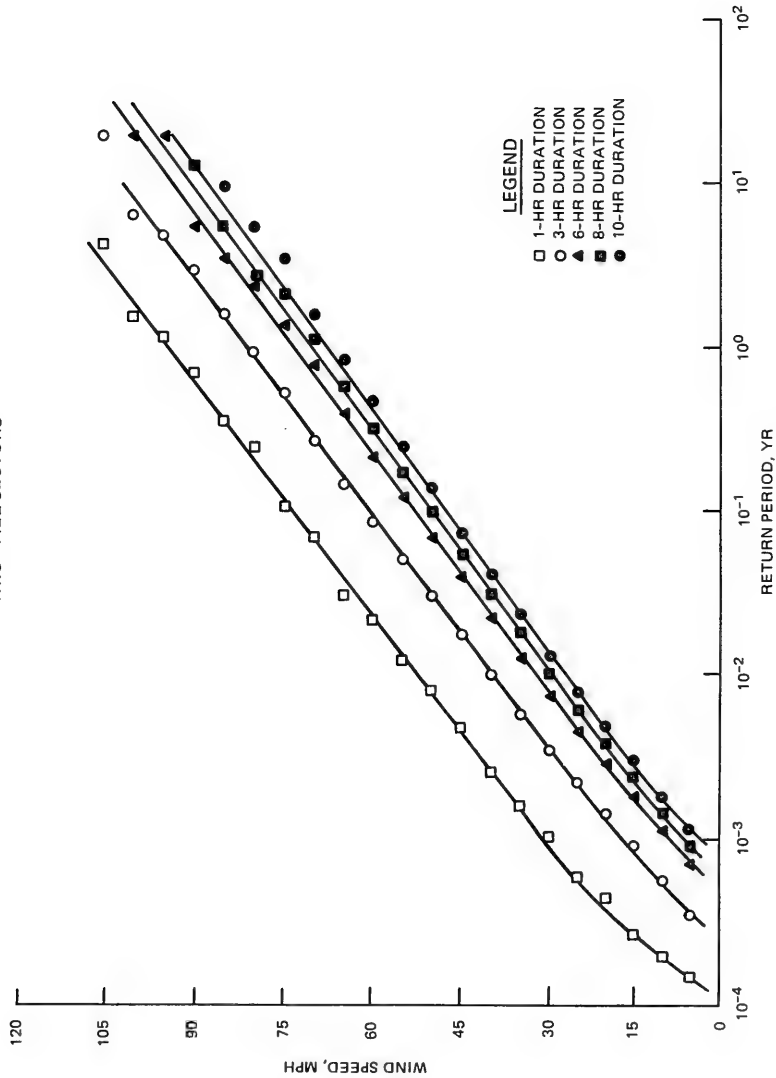● 10-HR DURATION

WIND SPEED, MPH

RETURN PERIOD, YR

Figure 19. Wind speed versus return period plot for NWS data

This correction is

$$\left(U_a\right)_{cor} = R_b U_a$$

where

$$R_b = \left\{ 1 + \frac{h\sigma \ln^2\left(\frac{L}{z_o}\right) u^o(x\,,\,z)}{L\ln\left(\frac{\ell}{z}\right)\left[\ln\left(\frac{z}{\ell}\right) + \ln\left(\frac{\ell}{z_o}\right)\right]} \right\}^{-1} \qquad (26)$$

in which

      h = height of the hill

      σ = 1.0

      L = factor of island length

      z_o = roughness length

      $\hat{u}^o$ = dimensionless quantity representing the perturbation of the upwind velocity due to the presence of the hill

      z = anemometer height above the island

      ℓ = thickness of the internal boundary layer

This correction assumes that L is much larger than h and that it is rural terrain. A maximum correction of 0.65 was applied in the direction of the short axis of the island, and a minimum correction of 0.85 was applied in the direction of the long axis of the island. These corrections were made so wind data could be applied directly to wave forecasting curves.

Wind summary

    42. The same computer program used to analyze the NWS data was used for the Puffin Island data. Data were available for only the 3-hr averages, so summaries were produced for the 3- and 6-hr winds. Of the 4,800 observations, 17 percent were bad.

    43. The distribution of the hourly wind with respect to direction is shown as a wind rose (Figure 20). The wind rose shows the distribution of winds in 16 directional sectors as a percent of all winds. The bars are broken into 10-mph intervals.

    44. The short period of record for the data from Puffin Island anemometer makes it difficult to create reliable curves for wind speed and duration versus return period. The best use for this data is for comparison with the NWS data.
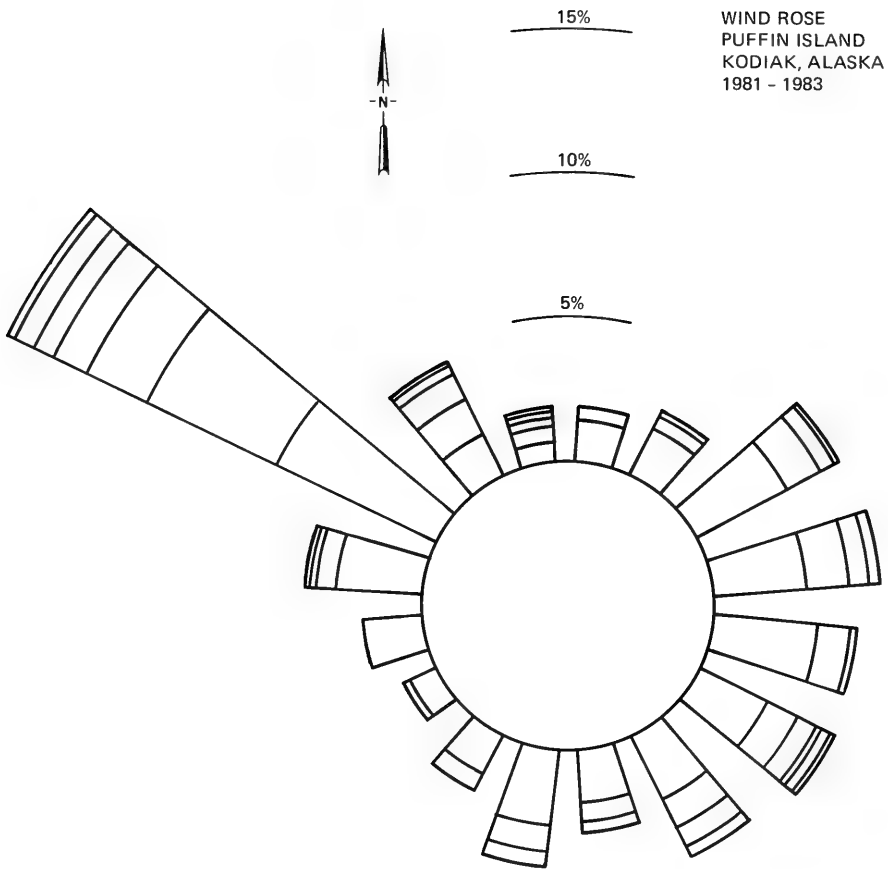
Figure 20.   Wind rose plot for Puffin Island data

Comparison of NWS and Puffin Island Data

45.   The Puffin Island data seem to compare well in velocity, direc-
tion, duration, and return period with the NWS data. Figure 21 shows the
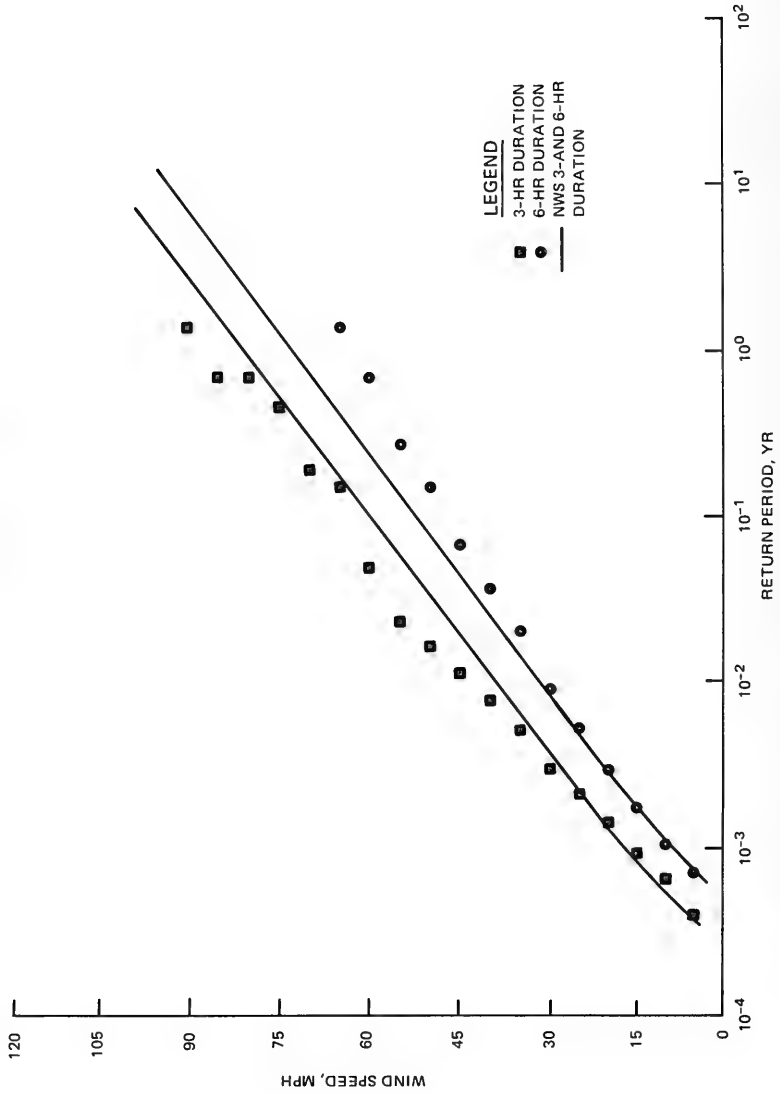distribution of wind speed and duration relative to return period (3- and

47

Figure 21. Wind speed versus return period for Puffin Island data

6-hr duration). The solid curves represent the distribution for the NWS data (see Figure 19). The Puffin Island data follow the NWS distribution closely in the lower parts of the curves. This is the region where the Puffin Island data are most reliable. This implies that the NWS wind data are a good estimate of the Puffin Island wind conditions which would give a good estimate of the open water conditions in St. Paul Harbor and Chiniak Bay at Kodiak. The following section presents the extremal analysis of the winds using the NWS wind data. The extremal curves are recommended for design purposes.

Analysis of Annual Maxima for NWS Data

46. The NWS data for 1-, 3-, 6-, 8-, 10-, 12-, 15-, 18-, 21-, 24-, 27-, and 30-hr wind speed averages were searched for yearly maxima for input to the extremal plotting routine, EXPLOT. The resulting plots are provided in Appendix C. It is apparent for all but the 1-hr averages that the smaller eight data points have been smoothed out and can no longer be considered extremes. For this reason the points in question were not used when fitting the least squares lines to the data, and therefore, do not affect the resulting extrapolated wind speeds. Table 18 contains a full listing of the predicted wind speeds for given return periods and hourly averages. The analysis was computed for all directions, the offshore exposure (45-180 deg relative to 0 deg from North) and Womens Bay (202.5-247.5 deg) separately as indicated in Appendix C and Table 18. The Extremal Type I or Fisher-Tippett I distribution was used in this analysis. The Fisher-Tippett or Extremal Type II distribution results were also computed and found to be unsatisfactory. In general, the chosen extremal model fits the data very well as is demonstrated by the plots.

Wave Forecasts Based on NWS Wind Data

47. The long-term (extremal) distributions of wind velocities averaged over varying durations for all directions for 247.5-292.5 deg (Womens Bay), and for 45-157.5 deg (Gulf of Alaska) are presented in Appendix C. This information can be used to derive equivalent significant wave heights and peak spectral periods, given appropriate assumptions of water depth and fetch. Two sectors of interest were defined which correspond to the 7-mile fetch of

49

Table 18

Maximum Windspeeds, Miles per Hour with

Hours Averaged and Return Period

Hours	Return Period, years						
Averaged	5	10	20	40	50	60	100
			All Directions				
1	94.0	103.4	112.4	121.3	124.1	126.4	132.9
3	80.1	89.2	98.0	106.5	109.2	111.5	117.7
6	74.0	83.1	91.8	100.3	103.1	105.3	111.5
8	70.9	79.4	87.5	95.5	98.0	100.1	105.9
10	68.4	76.8	85.0	92.9	95.4	97.5	103.3
12	49.3	56.2	62.3	68.3	70.2	71.8	76.1
15	46.2	52.3	58.2	64.0	65.9	67.4	71.6
18	44.8	50.5	56.1	61.5	63.2	64.6	68.6
21	42.9	48.4	53.6	58.7	60.4	61.7	65.4
24	41.5	47.2	52.6	57.9	59.6	61.0	64.8
27	37.8	41.8	45.6	49.3	50.5	51.5	54.2
30	36.9	41.4	45.7	50.0	51.3	52.4	55.5
			Offshore Exposure				
1	72.2	79.7	86.8	93.8	96.0	97.8	102.9
3	62.1	70.7	78.9	87.0	89.5	91.6	97.5
6	56.1	63.5	70.7	77.8	80.0	81.9	87.0
8	53.0	59.5	65.8	72.0	74.0	75.6	80.1
10	50.1	56.1	62.0	67.6	69.4	71.0	75.0
			Womens Bay				
1	52.5	61.7.	70.5	79.1	81.8	84.1	90.4
3	37.2	47.1	56.7	66.0	69.0	71.5	78.3
6	26.5	31.1	35.5	39.7	41.1	42.2	45.3
8	26.1	31.5	36.7	41.8	43.5	44.8	48.5
10	24.3	29.8	35.1	40.2	41.9	43.2	47.0

Womens Bay to Dog Bay, and the virtually unlimited fetch across the Gulf of
Alaska. The depths along the Womens Bay fetch vary from a few feet to over
50 ft. Shallow water forecasting curves (Vincent and Lockhart 1983) for an
assumed constant 35-ft depth and 7-mile fetch were used to translate veloc-
ities and durations at selected return periods from Figures C1-C5 to equiva-
lent significant wave heights and peak periods for the Womens Bay fetch, as
presented in Table 19. The fetch limitation makes the higher velocities of
1-hr duration the extreme condition in terms of wave height.

Table 19

Wave Forecast for Womens Bay Fetch Based on NWS Wind Data

Duration	Return Period, year						
hr	5	10	20	40	50	60	100
1	1.8, 4.2	2.0, 4.2	2.2, 4.7	2.6, 5.0	2.6, 9.0	2.7, 5.0	2.9, 5.2
3	1.1, 3.7	1.4, 4.0	1.7, 4.3	2.1, 4.6	2.3, 4.7	2.3, 4.8	2.5, 4.9

Note: First number under Return Period indicates Significant Wave Height, m;
second number indicates Peak Period, sec.

48. A similar translation of winds from the Gulf of Alaska (Figures C6-
C17) was performed using the deepwater forecasting curves with duration as the
only limitation. Table 20 indicates a duration of 24 hr as the extreme condi-
tions in this case with low probability deepwater significant wave heights

Table 20

Wave Forecast for Gulf of Alaska Based on NWS Wind Data

Duration	Return Period, year						
hr	5	10	20	40	50	60	100
12	5.5, 10.9	6.4, 11.4	7.3, 12.0	8.2, 12.6	8.5, 12.8	8.8, 13.0	9.1, 13.3
15	5.8, 11.7	6.7, 12.3	7.9, 13.1	8.8, 13.8	9.1, 14.0	9.5, 14.1	10.4, 14.8
18	6.7, 12.6	7.6, 13.4	8.5, 14.1	9.5, 14.7	10.1, 15.0	10.4, 15.1	11.0, 15.5
21	7.0, 13.3	8.2, 14.2	9.1, 15.0	10.4, 15.8	10.7, 15.9	11.0, 16.1	11.9, 16.6
24	7.0, 13.9	8.5, 14.6	10.1, 15.8	11.3, 16.4	11.6, 16.8	11.9, 16.9	12.8, 17.3
27	7.0, 14.2	8.2, 14.8	8.8, 15.5	9.8, 16.1	10.1, 16.3	10.4, 16.4	11.0, 17.0
30	6.7, 13.8	8.2, 15.3	9.8, 16.2	11.0, 17.0	11.3, 17.1	11.6, 17.2	12.5, 17.9

Note: First number under Return Period indicates Significant Wave Height, m; second number
indicates Peak Period, sec.

very close to those predicted using the WIS data base (see Table 21). The
duration over 21 hr for the low probability events have corresponding fetches
on the order of 300 to 400 nautical miles. Though no physical barriers to the
wind exist, this distance is on the scale of the synoptic weather patterns.
The variations of velocity across weather patterns of this scale are modeled
by the WIS data base, but are not using the NWS point source of data. This
inadequacy, along with the other measurement errors inherent in land-based
anemometers, indicates that the statistics from the WIS data base are more
reliable, as applied here, for wave conditions at Kodiak.

Table 21

Comparison of Extremes Predicted

from WIS Hindcast Data and

NWS Wind Data Analysis

Return Period	Significant Wave Height, m	
years	WIS	NWS
5	9.92	7.0
10	10.6	8.5
20	11.28	10.1
40	11.95	11.3
50	12.17	11.6
60	12.35	11.9
100	12.84	12.8

49. The outer buoy location water depth is about 77 m. For linear waves with periods of 12 sec and longer, this does not constitute deep water. The deepwater assumption holds for h/Lo > 0.5 where h = water depth and Lo = deepwater wavelength. Values for h/Lo with h = 77 m and periods of 12 sec and longer are h/Lo < 0.34 ; thus, the waves traveling from deep water will be somewhat affected by the water depth. Corrections for this are available in wave tables (Skovgaard et al. 1974) that report the ratio of wave height to deepwater wave height as a function of h/Lo . Values for this ratio are listed in Table 22 for the range of wave periods of interest. Wave breaking limits were computed using a controlling depth of 7.5 m for the area between Puffin Island and Popov Island. It was found that for the extreme waves of this study the attenuation factor does not need to be modified using an upper limit of significant wave height.

Table 22

Ratio of Wave Height Over Deepwater

Wave Height for a Water Depth

of 77 m Versus Wave Period

Wave Period sec	$\dfrac{H}{Ho}$
14.0	0.932
14.3	0.929
14.5	0.929
14.8	0.926
15.0	0.923
15.3	0.920
15.5	0.920
15.8	0.918
16.0	0.916
16.3	0.916
16.5	0.914
16.8	0.914
17.0	0.913

50. The peak wave period that most accurately represents the local weather conditions comes from the WIS hindcast data set. The WIS hindcast period for the 20-year event is 14.3 sec. This value is also sufficient for

the 50- and 100-year wave conditions. The ratio of wave height in 77 m of water to deepwater wave height for waves with 14.3-sec periods is 0.929; thus, the 50- and 100-year deepwater significant wave heights given in Table 7, 12.17 and 12.84, respectively, will be 11.3 and 11.9 m at the outer buoy location.

51.   The WIS hindcast data applicable to Chiniak Bay were surveyed
for extreme wave conditions.   The resulting 62 significant wave heights were
found to fit the Extremal Type I distribution.   The resulting extrapolated
significant wave heights are reported in Table 7.   The associated reliability
analysis indicates that if the Extremal Type I is the proper model, then the
standard error in estimating the extremes is about one-tenth of a meter.   It
should be stressed that the major source of error is due to the choice of the
model and is thus not included in this number.

52.   Measured data from the area were also found to fit an Extremal
Type I distribution.   The results from this analysis tend to underestimate
long-term conditions such as the 10- to 50-year events.   This is mostly due
to the short data record length (2 years).   Extremes computed using the NWS
wind data are similar to those given by the hindcast analysis.   For the
50-year event they differ by about six-tenths of a meter, and for the
100-year event they are approximately the same.

53.   The peak wave period that most accurately represents the local
weather patterns is that computed by the WIS hindcast.   The wave period asso-
ciated with the 20-year extreme event is 14.3 sec.   This value should be suf-
ficient for the 50- and 100-year events as well.   The deepwater to intermedi-
ate water depth (77 m at the outer buoy) wave height correction for 14.3-sec
periods is 0.929.   This correction was applied to the significant wave
heights listed in Table 7 and the values listed in Table 23 were obtained.

Table 23

Depth Corrected to Outer Buoy (77 m) Significant

Wave Heights Versus Return Period

Return Period years	Significant Wave Height, m
5	9.22
10	9.85
20	10.48
40	11.10
50	11.31
60	11.47
100	11.93

54.   The deep- to shallow-water attenuation factor from Equation 25 is
0.374.   The values in Table 23 multiplied by this factor result in the inner-
buoy or shallow water extreme values given in Table 24.

Table 24

Attenuated Significant Wave Heights

Versus Return Period

Return Period years	Significant Wave Height, m
5	3.45
10	3.68
20	3.92
40	4.15
50	4.23
60	4.29
100	4.46

The values given in Table 24 along with the wave period of 14.3 sec are the
estimates for the long-term extreme events pertaining to the St. Paul Harbor
area, based on analyses of all the currently available data.

REFERENCES

Abramowitz, M., and Stegun, I. A. 1972. Handbook of Mathematical Functions, Dover, N. Y.

Borgman, L. E. 1963 (Aug). "Risk Criteria," Journal, Waterway, Port, Coastal and Ocean Division, American Society of Civil Engineers, Vol 89, No. WW3.

_____. 1982. "Extremal Analysis of Wave Hindcasts for the Diablo Canyon Area, California," report prepared by L. E. Borgman, Inc.

Borgman, L. E., and Resio, D. T. 1982. "Extremal Statistics in Wave Climatology," Topics in Ocean Physics, LXXX Corso, Soc. Italiana di Fisica, Bologna, Italy.

Carter, D. J. T., and Challenor, P. G. 1978. "Return Wave Heights at Seven Stones and Famita Estimated from Monthly Maxima," Report No. 66, Institute of Oceanographic Sciences.

Challenor, P. G. 1982. "A New Method for the Analysis of Extremes Applicable to One Years' Data," Report No. 142, Institute of Oceanographic Sciences.

Corson, W. D., and Resio, D. T. 1981 (May). "Comparisons of Hindcast and Measured Deepwater, Significant Wave Heights," WIS Report 3, US Army Engineer Waterways Experiment Station, Vicksburg, Miss.

Isaacson, M., and MacKenzie, N. O. 1981 (May). "Long Term Distributions of Ocean Waves: A Review," Journal, Waterway, Port, Coastal and Ocean Division, American Society of Civil Engineers, Vol 107, No. WW2.

Miller, I., and Freund, J. F. 1977. Probability and Statistics for Engineers, 2d ed., Prentice-Hall, Englewood Cliffs, N. J.

Petrauskas, C., and Aagaard, D. M. 1971. "Extrapolation of Historical Storm Data for Estimating Design Wave Heights," Journal, Society of Petroleum Engineering, Vol 11.

Ragsdale, D. S. 1983 (Aug). "Sea State Engineering Analysis System (SEAS)," WIS Report 10, US Army Engineer Waterways Experiment Station, Vicksburg, Miss.

Simiu, E., and Scanlan, R. H. 1978. "Wind Effects on Structures," An Introduction to Wind Engineering, Wiley, New York.

Skovgaard et al. 1974. "Sinusoidal and Cnoidal Gravity Waves Formulae and Tables," ISVA Technical University of Denmark.

US Army Engineer District, Alaska. 1983a. "Alaska Coastal Data Collection Program (ACDCP)," Report 1, State of Alaska Department of Transportation and Public Facilities, Anchorage, Alaska.

_____. 1983b. "Alaska Coastal Data Collection Program (ACDCP)," Report 2, State of Alaska Department of Transportation and Public Facilities, Anchorage, Alaska.

US Army Engineer Waterways Experiment Station. 1981 (Mar). "Method of Determining Adjusted Windspeed: VA, for Wave Forecasting," CETN-I-5, Vicksburg, Miss.

_____. 1984. Shore Protection Manual (2 vols), 4th ed., Vicksburg, Miss.

Vincent, C. L., and Lockhart, J. H., Jr. 1983 (Sep). "Determining Sheltered Water Wave Characteristics," ETL 1110-2-305, Department of the Army, Office, Chief of Engineers, Washington, DC.

Wang, S., and LeMéhauté, B. 1983 (May). "Duration of Measurements and Long Term Wave Statistics," Journal, Waterway, Port, Coastal and Ocean Engineering, American Society of Civil Engineers, Vol 109, No. 2.

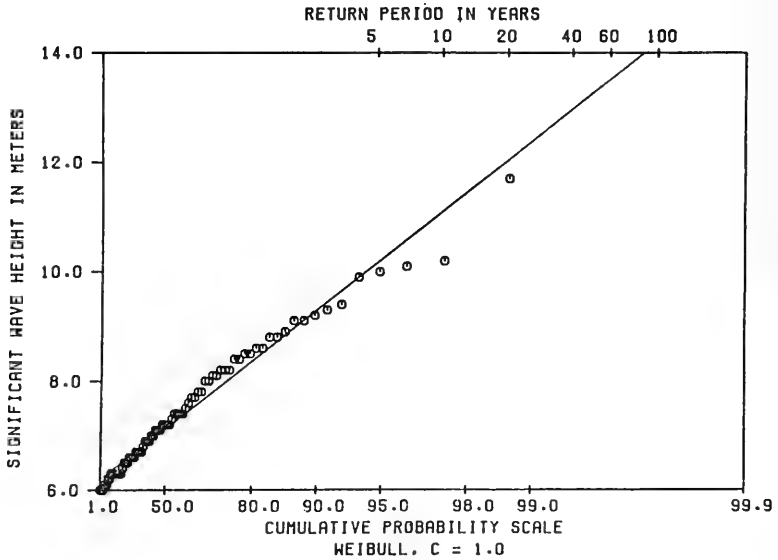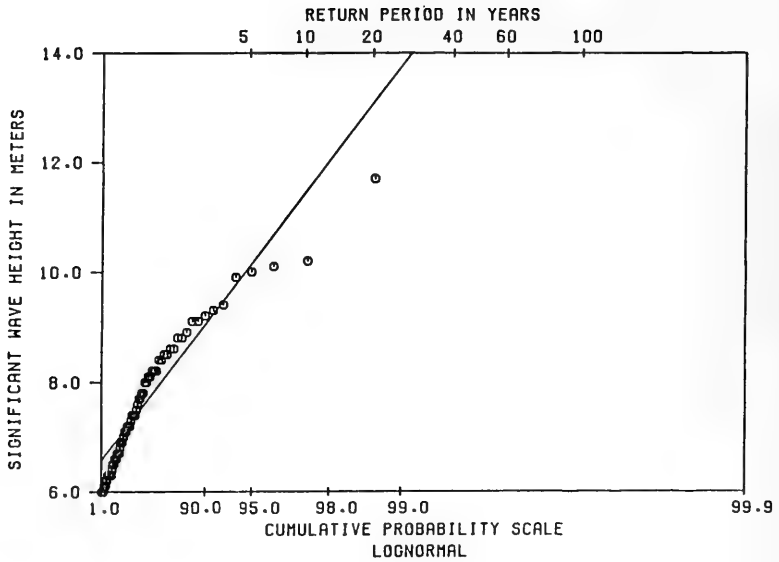APPENDIX A: KODIAK STORM DATA, 1956-1975

Kodiak Storm Data

Date	H_{SMAX}, m	Period sec
01-18-56	6.20	12.50
01-28-58	8.80	12.50
02-12-58	6.60	11.10
02-24-58	6.90	11.10
11-20-58	7.80	11.10
12-10-58	6.30	10.00
01-16-59	11.70	14.30
01-21-59	7.20	10.00
11-16-59	7.40	11.10
01-31-60	9.90	14.30
02-07-60	8.90	14.30
10-24-60	7.50	11.10
11-22-60	7.00	11.10
12-20-60	6.70	11.10
01-19-61	9.20	12.50
01-24-61	6.20	11.10
11-26-61	6.30	11.10
10-27-62	8.10	12.50
11-07-62	6.30	11.10
11-23-62	7.20	10.00
11-28-62	6.30	10.00
12-30-62	6.00	11.10
02-08-63	8.40	12.50
10-21-63	6.80	11.10
10-31-63	9.30	12.50
11-11-63	6.70	14.30
11-22-63	6.50	12.50
11-25-63	7.20	11.10
12-21-63	8.50	11.10
01-12-64	6.90	11.10
01-24-64	6.60	10.00
01-20-64	9.40	12.50
12-01-64	8.20	12.50
10-02-65	6.30	11.10
10-05-65	7.60	11.10
01-13-66	7.30	12.50
01-26-66	8.60	12.50
11-01-66	7.40	11.10
01-10-67	7.10	14.30
02-27-67	6.00	12.50

(Continued)

Date	H_{SMAX}, m	Period sec
12-02-67	6.30	12.50
12-07-67	6.00	12.50
12-23-67	7.70	14.30
01-16-68	6.60	12.50
01-22-68	6.50	10.00
03-21-68	6.90	14.30
11-04-68	7.70	11.10
11-18-68	8.20	11.10
11-28-68	6.70	10.00
12-14-68	7.40	12.50
02-07-69	6.40	10.00
02-11-69	6.10	11.10
10-11-69	7.10	10.00
11-19-69	6.50	11.10
12-02-69	8.50	12.50
12-19-69	8.80	12.50
12-23-69	9.10	12.50
01-20-70	8.00	11.10
10-31-70	6.30	11.10
11-11-70	9.10	12.50
01-17-71	6.60	14.30
01-15-72	6.70	12.50
03-09-72	7.20	11.10
11-25-72	10.20	14.30
12-17-72	7.00	14.30
12-24-72	10.10	14.30
01-27-73	7.80	14.30
12-06-73	6.10	12.50
12-13-73	6.30	12.50
12-19-73	8.60	14.30
12-23-73	7.10	10.00
12-27-73	10.00	12.50
01-17-74	8.00	14.30
04-13-74	6.10	11.10
10-30-74	8.40	14.30
01-12-75	7.40	14.30
11-19-75	8.20	12.50
12-21-75	8.10	11.10

A3

APPENDIX B: DATA PLOTS FOR PROPOSED EXTREMAL MODELS

RETURN PERIOD IN YEARS

LOGNORMAL

RETURN PERIOD IN YEARS

WEIBULL, C = 1.0

B2

RETURN PERIOD IN YEARS

CUMULATIVE PROBABILITY SCALE
EXTREMAL TYPE I

RETURN PERIOD IN YEARS

CUMULATIVE PROBABILITY SCALE
EXTREMAL TYPE I

B3

RETURN PERIOD IN YEARS
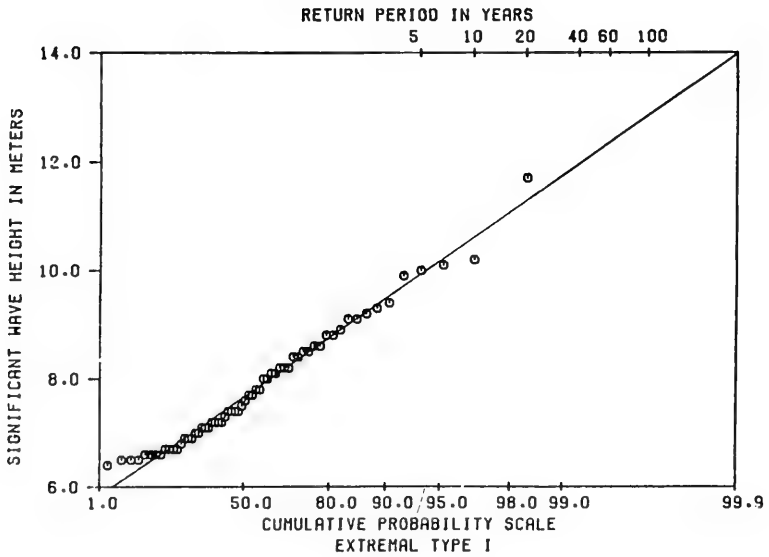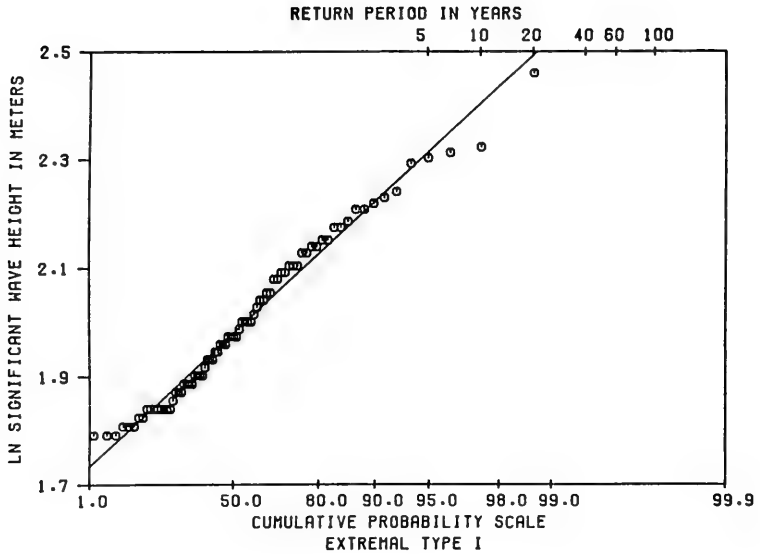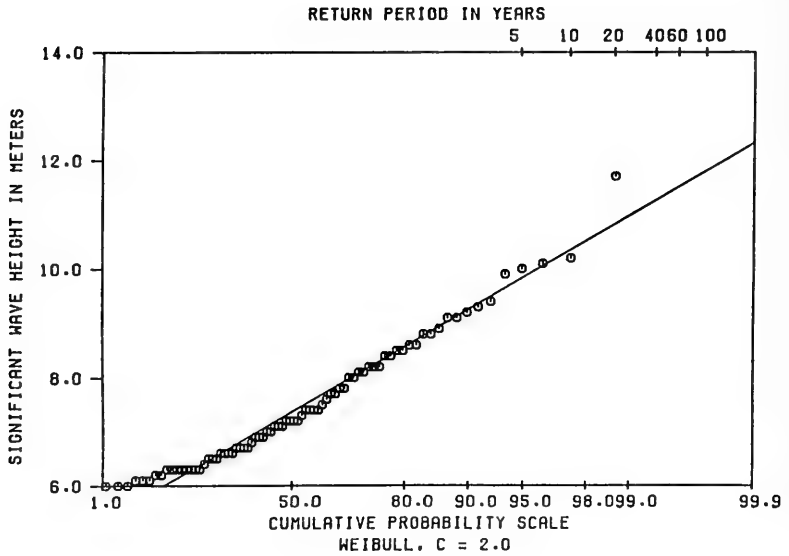
APPENDIX C: EXTREMAL DISTRIBUTIONS OF WIND VELOCITIES
FOR WOMENS BAY AND GULF OF ALASKA
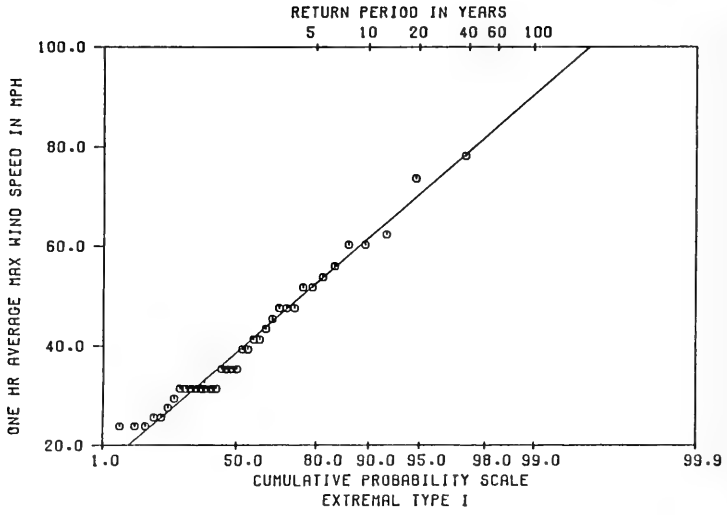
Figure C1.   Womens Bay, 1-hr averages
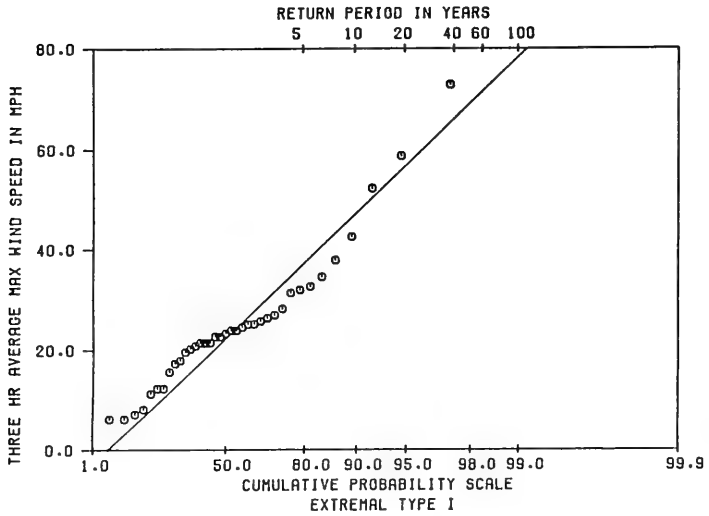
Figure C2.   Womens Bay, 3-hr averages
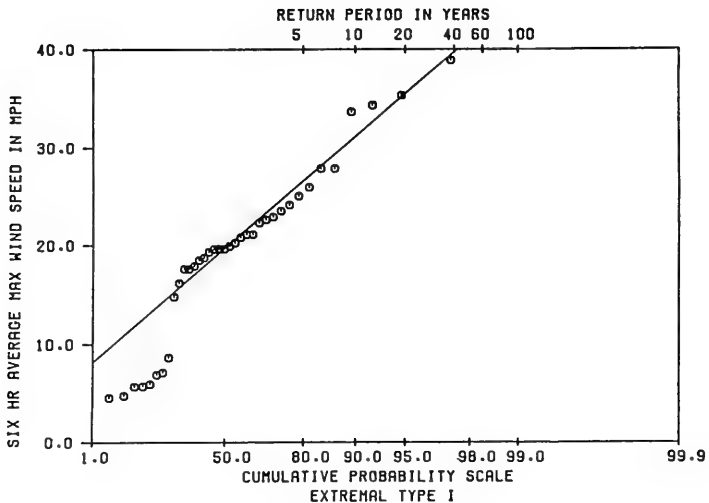
Figure C3.   Womens Bay, 6-hr averages
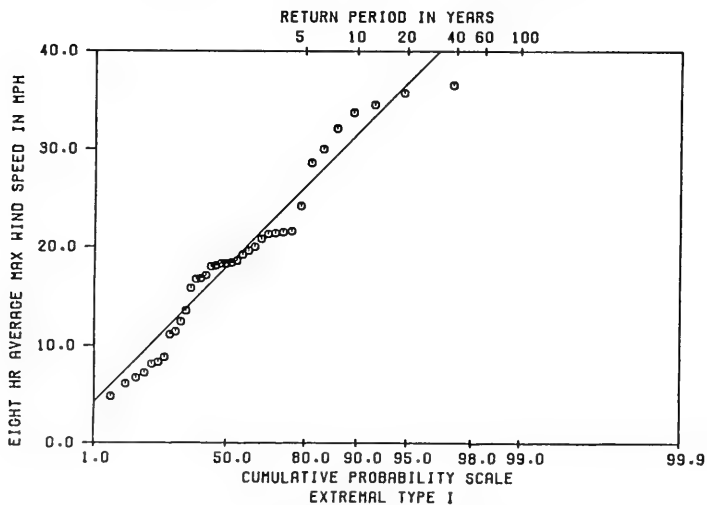
Figure C4.   Womens Bay, 8-hr averages
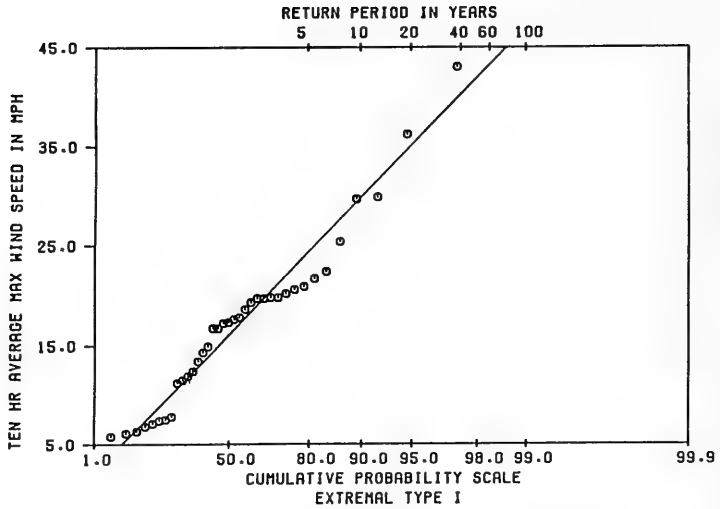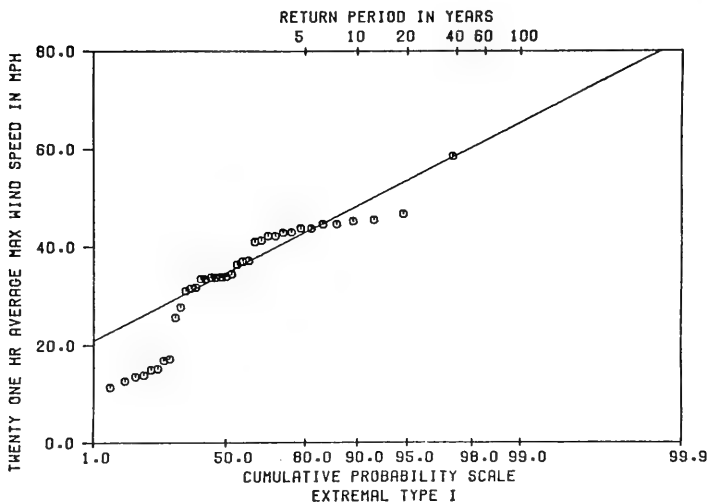
Figure C5. Womens Bay, 10-hr averages
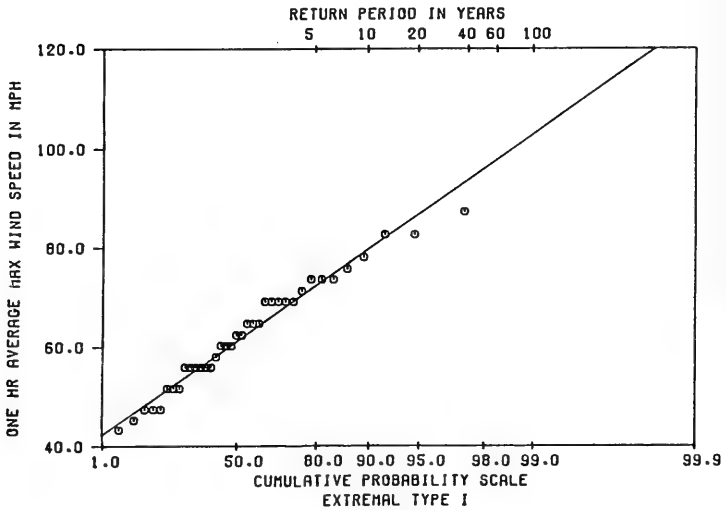
Figure C6. Gulf of Alaska, 1-hr averages
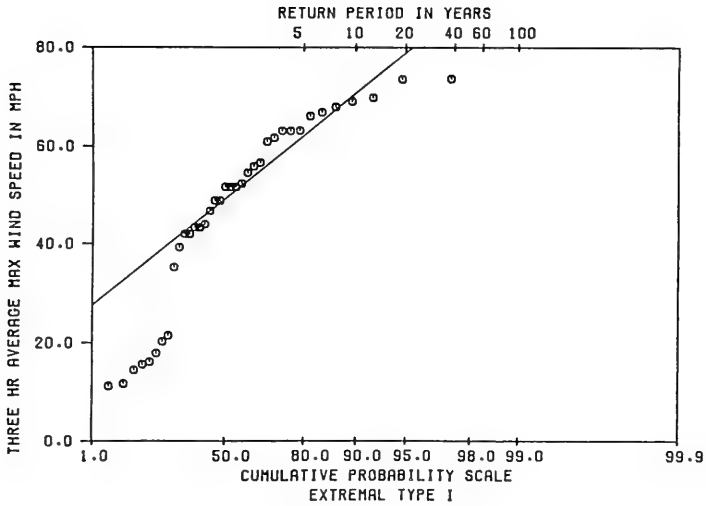
Figure C7. Gulf of Alaska, 3-hr averages
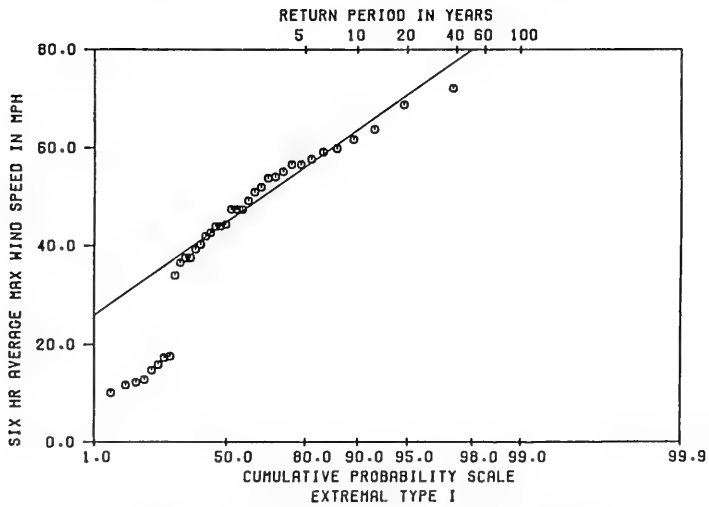
Figure C8. Gulf of Alaska, 6-hr averages

C5
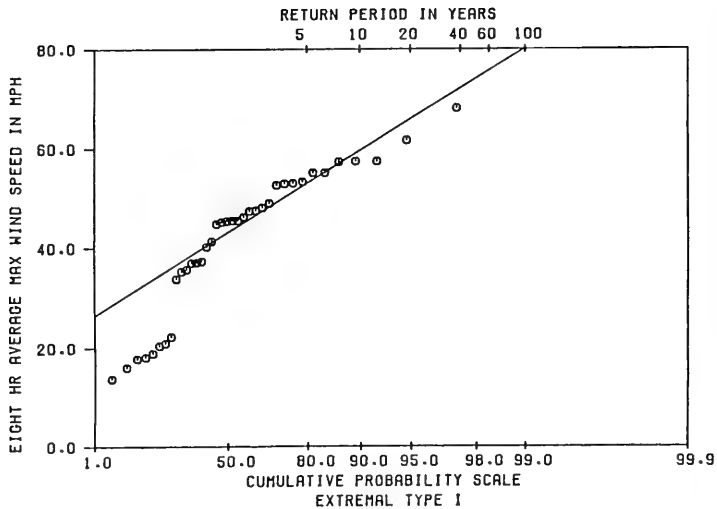
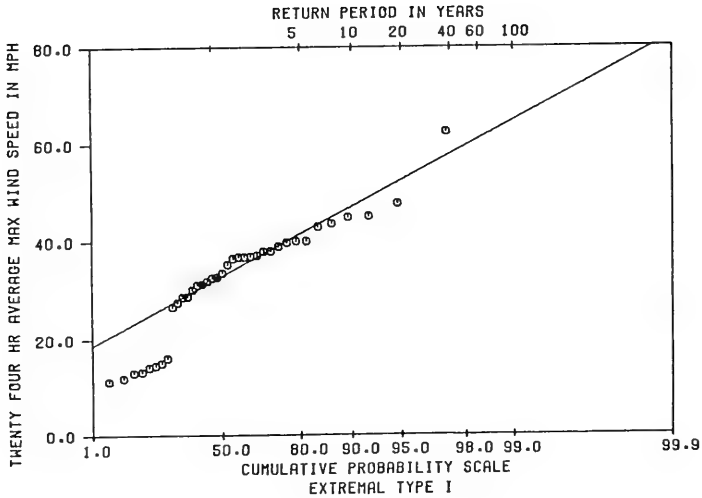Figure C9. Gulf of Alaska, 8-hr averages
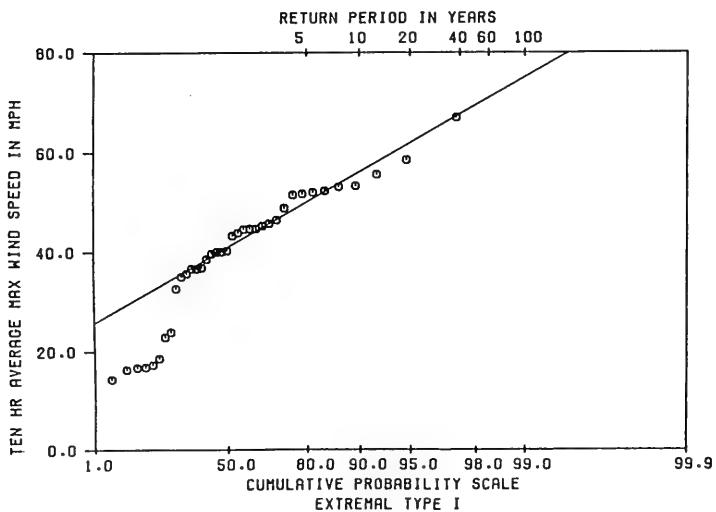
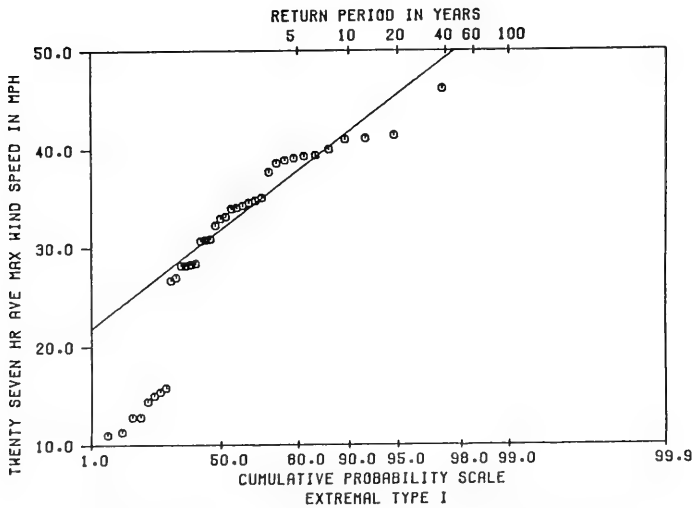Figure C10. Gulf of Alaska, 10-hr averages
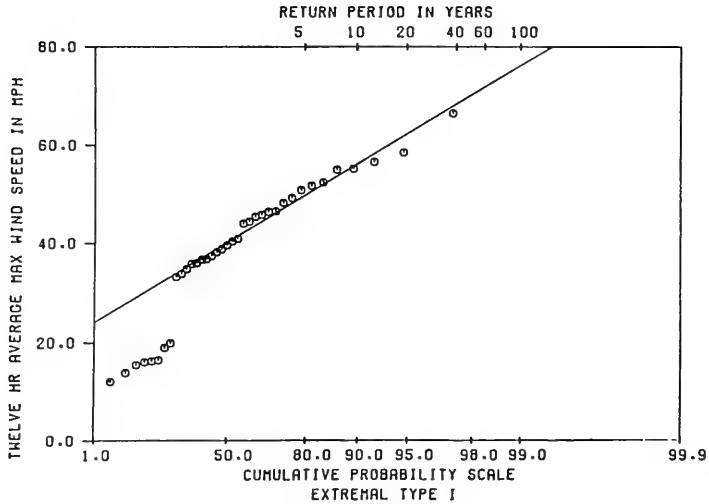
Figure C11. Gulf of Alaska, 12-hr averages
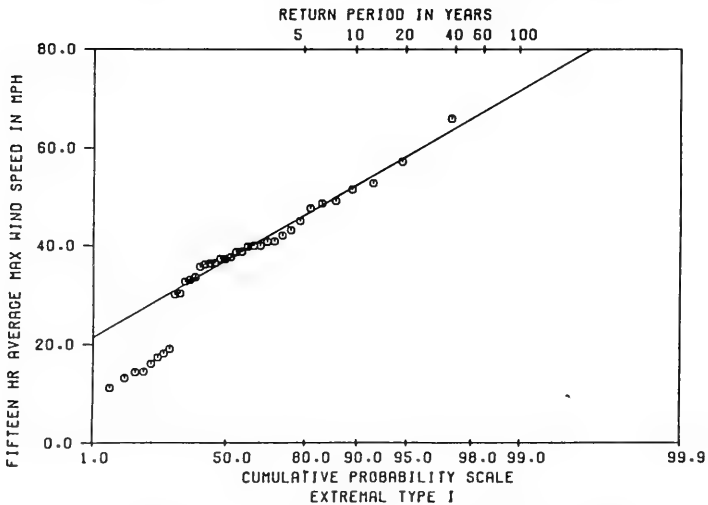
Figure C12. Gulf of Alaska, 15-hr averages

C7
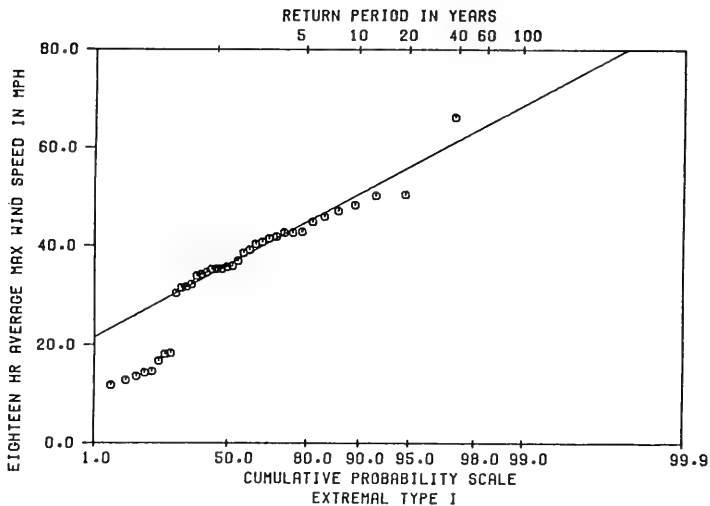
Figure C13. Gulf of Alaska, 18-hr averges

Figure C14. Gulf of Alaska, 21-hr averages

C8

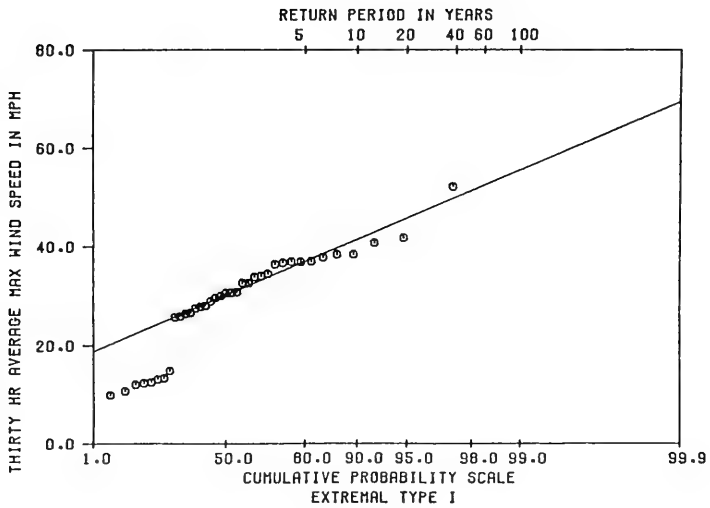Figure C15.   Gulf of Alaska, 24-hr averages

Figure C16.   Gulf of Alaska, 27-hr averages

C9

Figure C17. Gulf of Alaska, 30-hr averages